# ORIGINAL RESEARCH

Colorectal Cancer Cells Adhere to and Migrate Along the Neurons of the Enteric Nervous System

Emilie Duchalais,[1,2,3] Christophe Guilluy,[2,4] Steven Nedellec,[2,5] Melissa Touvron,[1] Anne Bessard,[1,2] Yann Touchefeu,[1,2] Céline Bossard,[2,6] Hélène Boudin,[1,2] Guy Louarn,[2,7] Michel Neunlist,[1,2,§] and Laurianne Van Landeghem[1,2,8,§]

[1]Inserm U1235, Institut des Maladies de l'Appareil Digestif, Nantes, France; [2]Université de Nantes, Nantes, France; [3]Clinique de Chirurgie Digestive et Endocrinienne, Centre Hospitalier Universitaire de Nantes, Institut des Maladies de l'Appareil Digestif, Nantes, France; [4]Inserm UMR 1087, Nantes, France; [5]Micropicell, Nantes, France; [6]Service d'Anatomie et Cytologie Pathologiques, Centre Hospitalier Universitaire de Nantes, France; [7]Institut des Matériaux Jean Rouxel, Centre National de la Recherche Scientifique, Nantes, France; [8]Department of Molecular Biomedical Sciences, College of Veterinary Medicine, North Carolina State University, Raleigh, North Carolina
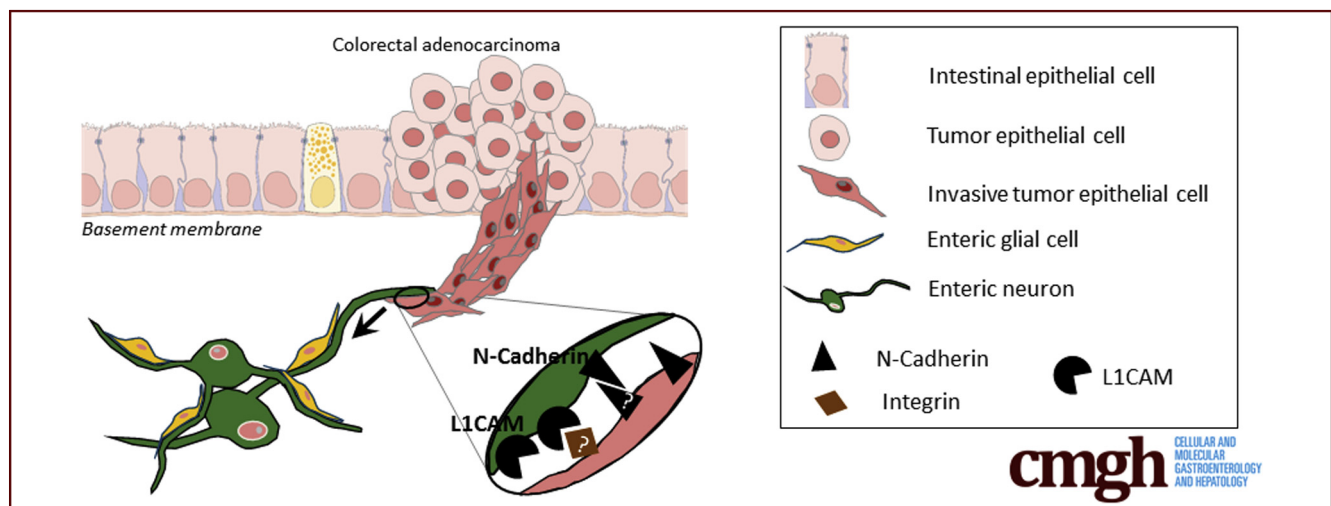
SUMMARY

These findings show that colorectal cancer cells adhere to and migrate along enteric neurons partly via L1CAM and N-cadherin. Thus, the dense network of local enteric neurons in the tumor microenvironment may serve as the local route for colorectal cancer spreading.

BACKGROUND & AIMS: In several types of cancers, tumor cells invade adjacent tissues by migrating along the resident nerves of the tumor microenvironment. This process, called *perineural invasion*, typically occurs along extrinsic nerves, with Schwann cells providing physical guidance for the tumor cells. However, in the colorectal cancer microenvironment, the most abundant nervous structures belong to the nonmyelinated intrinsic enteric nervous system (ENS). In this study, we investigated whether colon cancer cells interact with the ENS.

METHODS: Tumor epithelial cells (TECs) from human primary colon adenocarcinomas and cell lines were cocultured with primary cultures of ENS and cultures of human ENS plexus explants. By combining confocal and atomic force microscopy, as well as video microscopy, we assessed tumor cell adhesion and migration on the ENS. We identified the adhesion proteins involved using a proteomics approach based on biotin/streptavidin interaction, and their implication was confirmed further using selective blocking antibodies.

RESULTS: TEC adhered preferentially and with stronger adhesion forces to enteric nervous structures than to mesenchymal cells. TEC adhesion to ENS involved direct interactions with enteric neurons. Enteric neuron removal from ENS cultures led to a significant decrease in tumor cell adhesion. TECs migrated significantly longer and further when adherent on ENS compared with on mesenchymal cells, and their trajectory faithfully followed ENS structures. Blocking N-cadherin and L1CAM decreased TEC migration along ENS structures.

CONCLUSIONS: Our data show that the enteric neuronal network guides tumor cell migration, partly via L1CAM and N-cadherin. These results open a new avenue of research on the underlying mechanisms and consequences of perineural invasion in colorectal cancer. *(Cell Mol Gastroenterol Hepatol 2018;5:31–49; https://doi.org/10.1016/j.jcmgh.2017.10.002)*

Keywords: Colorectal Cancer; Enteric Neurons; Adhesion; Migration.

Resident and recruited cells in the vicinity of cancer cells, which comprise the so-called *tumor microenvironment*, have a leading role in regulating tumor growth and spreading. These cells engage in cross-talk with tumor cells via paracrine signaling or direct cell–cell interactions, resulting in bidirectional remodeling in favor of tumor cell proliferation and migration.[1] For instance, extracellular matrix reorganization orchestrated by tumor cells and fibroblasts provides stiffened fibrils to guide the migration of tumor cells and favor tumor invasion.[2] Several studies also have shown that tumor cells can migrate directly along specific resident cells of the microenvironment using membrane and surface adhesion molecules for physical and molecular guidance, respectively.[3,4] Currently, only a few cell types of the tumor microenvironment have been shown to provide such physical guidance. These include cancer-associated fibroblasts during collective invasion, endothelial cells during tumor cell intravasation, and Schwann cells during perineural invasion.[3,5,6]

Perineural invasion, defined as tumor cell invasion along nerves, is one of the main routes for cancer dissemination and metastatic spread in pancreatic and prostate cancers.[7] In colorectal cancer, histologic characterization of invasive adenocarcinomas has shown the presence of tumor epithelial cell (TEC) nests in close proximity to the intrinsic nervous system of the colon and rectum, called the enteric nervous system (ENS).[8,9] Indeed, tumor cell nests have been found surrounding S-100β–positive glial cell structures located in the myenteric plexus.[9] Similar to the term given in pancreatic and prostate cancers, the presence of TECs surrounding ENS structures has been called *perineural invasion*. Although such perineural invasion in the ENS plexus can be a risk factor for shortened survival in colorectal cancer patients,[9] whether and how colorectal cancer cells physically interact with the ENS components has not been explored.

Colorectal neural cells that belong to the intrinsic ENS are organized into several dense ganglionated networks, or plexi, distributed throughout the digestive wall along the whole colon and rectum.[10,11] The ENS is composed of enteric neurons surrounded by specific glial cells, called *enteric glial cells*. Unlike other peripheral nerves, all enteric neurons of the ENS are unmyelinated and are not ensheathed by perineurium or endoneurium layers.[12] Importantly, because enteric glial cells do not completely cover enteric neurons, the neuronal membrane is exposed to direct interactions with the cells of the microenvironment. In healthy colon and rectum, the ENS communicates with colorectal epithelial cells predominantly via indirect paracrine bidirectional interactions through the basement membrane.[13] For instance, epithelial cells release neurotrophic factors favoring neuronal survival,[14] and the ENS regulates the proliferation and differentiation of epithelial cells via the secretion of various neurogliomediators.[15–18] In colorectal cancer, drastic rearrangement of the colonic or rectal mucosa and resulting disruption of the basement membrane can facilitate tumor cell invasion into surrounding tissues. This process may be enhanced owing to direct cellular contact between tumor cells and enteric nervous structures.

In pancreatic and prostate cancers, the perineural dissemination route involves direct and indirect interactions between nerves and tumor cells. These reciprocal interactions include chemoattraction between Schwann cells and tumor cells, nerve-induced tumor cell proliferation, and tumor cell–induced neuritogenesis.[19–22] In addition, in myelinated peripheral nerves, tumor cells have been shown to adhere to the extracellular matrix of perineural sheaths and directly to the membrane of myelinating Schwann cells.[5,23] Several studies have directly shown tumor cell migration along autonomous and somatic nerves in in vitro cocultures of tumor cells and sciatic nerves or mouse dorsal root ganglia,[5,21,22,24] and in vivo after subcutaneous or perisciatic injection of tumor cells.[5,21,25] However, whether TECs can physically adhere to and migrate along nonmyelinated intrinsic nervous structures remains unknown. This open question is particularly relevant in the colorectal cancer field because the most abundant resident neural cells in this tumor microenvironment belong to the nonmyelinated ENS. Therefore, here we used confocal, time-lapse, and atomic force microscopy to test the hypothesis that TECs adhere to and migrate along enteric neurons. By using a novel biochemical assay, we identified N-cadherin and L1CAM as proteins that are involved in ENS/TEC physical interactions. Finally, we confirmed our main findings using human explant cultures of submucosal plexus and human primary tumor cells isolated from adenocarcinomas from colorectal cancer patients.

Materials and Methods
Human Primary Colorectal Adenocarcinoma Collection

All primary human colorectal adenocarcinoma samples used in the study were obtained from colorectal cancer surgical specimens (Authorization no. DC-2008-402). Informed consent was obtained for all included patients. Colorectal cancer samples were used for histology and primary human tumor cell isolation. Of note, macroscopically healthy colon segments taken at a distance of at least 10 cm from the tumor were used for ex vivo culture of human submucosal plexus.

Cell and Organotypic Culture
Cell lines. The human colorectal cancer Caco-2 cell line, the IEC6 non transformed rat intestinal epithelial cell line, and the A7R5 smooth muscle cell line were originally from American Type Culture Collection (Manassas, VA). All cell

lines were cultured at 37°C with 5% CO_2 in Dulbecco's modified Eagle medium (DMEM) medium containing 10% fetal calf serum, 2 mmol/L glutamine, 50 μg/mL streptomycin, and 50 U/mL penicillin (Invitrogen, Carlsbad, CA). Cells were passaged when they reached 70% confluence. Caco-2, IEC-6, and A7R5 cell lines were used at 10–60, 10–30, and 11–18 passages, respectively. All cell lines were confirmed routinely to be mycoplasma free using polymerase chain reaction testing.

Primary human TECs. Primary human TECs were isolated from colorectal adenocarcinoma surgical specimens. Tumor samples were collected in Krebs medium and subsequently sliced into 2-mm^3 pieces in DMEM containing 10% fetal calf serum. Tumor pieces were placed successively in a 6.5 mmol/L dithiothreitol solution at room temperature and an enzymatic digestion solution containing 0.25 μg/mL amphotericin B, 20 mmol/L HEPES, 150 μg/mL DNase1, and 250 μg/mL collagenase I at 37°C. After enzymatic inhibition and filtration, red cells were removed using a lysing buffer (RUO; BD Biosciences, San Jose, CA). Remaining cells then were suspended in DMEM-F12 (1:1) medium (Invitrogen) containing 0.1% fetal calf serum, 50 μg/mL streptomycin, 50 U/mL penicillin, and 1% N-2 supplement (Life Technologies).

Primary culture of ENS. Primary culture of ENS (pcENS) were obtained as previously described.[26] Neurons were removed from pcENS by successively passaging mature pcENS. After each passage, cells were plated at 5.5×10^4 cells/cm. After 2 passages, pcENS at confluence contained less than 0.05% neurons. The enteric glial cell line JUG2 was obtained from pcENS as previously described.[16]

Primary culture of enteric neurons. Enteric neuron primary cultures were obtained as previously described[27] from intestines of 15-day-old rat embryos using the same cell suspensions as for pcENS cultures. Cells were plated at 175,000 cells/cm on glass coverslips coated with poly-L-lysine (1 mg/mL; Sigma, St. Louis, MO) in DMEM containing 10% fetal calf serum, 2 mmol/L glutamine, 50 μg/mL streptomycin, and 50 U/mL penicillin (Invitrogen). Coverslips were transferred 3 hours later to wells containing enteric glial feeders in a way that avoids direct contact between the coverslip and the feeder layer. The glial feeder layer consisted of the enteric glial cell line JUG2. JUG2 was plated 4 days before transferring the coverslips at a density of 7500 cells/cm in DMEM containing 10% fetal calf serum, 2 mmol/L glutamine, 50 μg/mL streptomycin, and 50 U/mL penicillin (Invitrogen). After transfer, coverslips were cultured for 8 days on glial cell feeder layers in serum-free Neurobasal B27 medium (Gibco, Carlsbad, CA).

Ex vivo culture of human submucosal and myenteric plexus. Human submucosal plexi explants were prepared from areas of colon surgical specimens harvested at least 10 cm from the colorectal adenocarcinoma margin. Colon samples were whole-mount microdissected. The submucosa with the submucosal plexus and longitudinal muscle myenteric plexus were pinned in a sterile Sylgard-coated dish containing DMEM-F12 complete medium (Invitrogen) supplemented with 0.1% fetal calf serum, 100 UI/mL penicillin, 100 μg/mL streptomycin, 1.1 μg/mL amphotericin B, 6 mmol/L glutamine, and 2.1 g/L NaHCO3 for 4 hours.

Tumor epithelial cell and ENS co-culture. Single-cell suspensions of Caco-2 or primary human epithelial cells were added to confluent primary cultures of ENS or to human submucosal plexus explants at 2.1×10^4 cells/cm^2 in DMEM-F12 (1:1) medium containing 0.1% fetal calf serum, 50 μg/mL streptomycin, 50 U/mL penicillin, and 1% N-2 supplement (Life Technologies). For antibody blocking experiments, pcENS were pretreated with anti-L1CAM (clone UJ127, 4 μg/L, ab3200; Abcam, Cambridge, UK), anti–N-cadherin (clone GC-4, 10 μg/mL, C3865; Sigma), or mouse IgG as a nonblocking isotype control (10 μg/mL, Abcam). To evaluate the proportion of TECs adhered to pcENS with or without enteric neurons, Caco-2 cell suspension was added at a density of 10^5 cells/cm.

Infection and generation of stable cell lines. The plasmid pRRLSINcPPT-hPGK-EGFP (from D. Trono, plasmid 122252; Addgene, Cambridge, MA) was modified to generate green fluorescent protein (GFP)-expressing Caco-2 cells. From this plasmid, the hPGK-EGFP fragment was excised by digesting at the 2 sites *Xho* I/*Kpn* I. A multiple cloning site (MCS) then was inserted in its place. In this plasmid, pRRLSINcPPTMCS, the 3057-bp–long form of the mouse β-tubulin III promoter (from the pMb6MREIYFP vector, a special gift from A. Spano[28]), and the 720-bp EGFP fragment were inserted at *Xho* I/*BamH* I and *BamH* I/*Sal* I, respectively, to generate the second plasmid used in this study: pRRLSINcPPTMCS-pTujL-EGFP. Lentivirus particles were generated using these plasmids by the cellular and molecular analysis platform (University of Angers, Angers, France).

The lentivirus pLenti-CMV-RFP-IRES-PURO-WPRE (a gift from Dr V. Trichet, UMR_S 957, University of Nantes, Nantes, France) was used to generate TurboRFP-positive Caco-2 cells. The lentivirus pLKO.1-puro-CMV-TagFP635 (plasmid SHC013V; Sigma) was used to generate FP635-positive IEC-6 cells. Caco-2 cells, IEC-6 cells, and pcENS were infected at a multiplicity of infection of 7.5. IEC-6 and Caco-2 cells infected with plKO.1-puro-CMV-TagFP635 and pLenti-CMV-RFP-IRES-PURO-WPRE were maintained under selection with 10 μg/mL puromycin. Caco-2 cells infected with pRRLSINcPPT-hPGK-EGFP were clonally selected according to GFP fluorescence and were maintained as 4 separate GFP-expressing Caco-2 cell clones.

Histology, Immunofluorescence, and Microscopy

Immunofluorescence and microscopy. Whole-mount dissected tissues and cell cultures were fixed with 4% paraformaldehyde in phosphate-buffered saline (PBS) at room temperature for 3 hours or 30 minutes, respectively. After permeabilization with PBS–sodium azide containing 10% horse serum and 1% Triton X (Sigma), tissues and cultures were incubated sequentially with primary and secondary antibodies. Paraffin-embedded tissues were baked at 60°C for 2 hours and then deparaffinized with successive incubation in xylene, absolute ethanol, 95% ethanol, and 70% ethanol. Tissue sections were incubated with antigen retrieval solution (Dako, Santa Clara, CA) at 110°C for 90 seconds. After cooling, sections were incubated successively in blocking solution (Dako) for 1 hour, followed by primary and

secondary antibodies diluted in antibody diluent solution (Dako) overnight at 4°C or 1 hour at room temperature, respectively. The following primary antibodies and dilutions were used for immunofluorescence microscopy experiments: mouse anti–tubulin III (Tuj) (1:200, T5076; Sigma), rabbit anti-Tuj (1:2000, ab18216; Abcam), rabbit anti–S-100β (1:500, IS504; Dako), goat α–smooth muscle actin (α-SMA) (1:200, ab21027; Abcam), mouse anti–α-SMA (1:500, ab7817; Abcam), mouse anti-L1CAM (1:500, ab24345; Abcam), rabbit anti–N-cadherin (1:200, ab12221; Abcam), mouse anti–epithelial cell adhesion molecule (EpCAM) (1:200, 324202; Biolegend, San Diego, CA), or rabbit anti-EpCAM (1:200, ab71916; Abcam). The following secondary antibodies were used: anti-mouse–Cy3 (1:500; Jackson ImmunoResearch, West Grove, PA), anti-mouse-FP488 (1:200; Interchim, Montluçon, France), anti-mouse–Alexa Fluor 647 (1:1000; Invitrogen), anti-rabbit–Alexa Fluor 647 (1:1000; Invitrogen), or anti-goat–Alexa Fluor 350 (1:1000; Invitrogen). Conventional microscope imaging of cell cultures was performed using an Axiozoom (Zeiss, Oberkochen, Germany) V16 microscope equipped with an Axiocam (Zeiss) HRm camera. Images were recorded with $1\times$/0.25 objective and processed with Zen software (Zeiss). Confocal microscope imaging of whole-mount dissected tissues, cell cultures, and histologic sections was performed using a Nikon (Tokyo, Japan) A1R confocal microscope, using appropriate laser wavelength and filters, with $60\times$/1.4 or $20\times$/0.75 objectives. Images were recorded with NIS (Nikon) software. Video microscopy was performed using a Leica DMI 6000B microscope equipped with a CCD coolsnap HQ2 camera (Photometrics, Tucson, AZ) in a 37°C, 5% CO_2 environment. Images were recorded with $20\times$/0.75 objective at a frequency of 1 image per 10 minutes.

Time-lapse acquisition analysis. Time-lapse acquisition analysis was performed with Metamorph (Molecular Devices, Sunnyvale, CA). The cell tracking option was applied to RFP-positive epithelial cells juxtaposed (or not) to enteric nervous structures. For quantification purposes, we defined cells juxtaposed to enteric nervous structures as RFP-positive cells overlapping with GFP-positive structures for at least the first 6 consecutive images, a 60-minute timeframe. We defined cells nonjuxtaposed to enteric nervous structures as RFP-positive cells that never overlapped with GFP-positive structures during the entire 12-hour acquisition. The total distance traveled and the distance to the origin of the tracked cells was calculated automatically by the software. Neuronal fiber and cell trajectory angles from the horizontal line also were determined automatically by the software after manual highlighting of the respective corresponding lines.

Adhesion assay. After co-incubation of epithelial cells (GFP-positive Caco-2 cells, primary human colorectal tumor cells, RFP-positive IEC-6) with pcENS, cells were fixed and stained, and then microphotographed with an Axiozoom V16 fluorescence microscope (Zeiss). Image analysis was performed using Fiji on the whole cell layer for all conditions, and the experimenter was blinded to treatment condition. Briefly, the fluorescent area corresponding to epithelial cells was converted to a mask and dilated to add 1

pixel to the edges of the mask. Epithelial cells were considered as juxtaposed to enteric neurons if at least 1 pixel of the dilated mask merged with an enteric neuron mask. Epithelial cell, enteric neuron, and myofibroblast fluorescent areas were measured using Fiji tools.

Adhesion strength measurement. To measure adhesion strength, we used an atomic force microscope (Nanowizard; JPK Instruments, Berlin, Germany) equipped with a CellHesion 200 module, mounted on a Zeiss microscope. All measurements were performed at 37°C using a Petri dish heater (JPK Instruments). After calibration, a tipless cantilever (Nanoworld Arrow TL1; 0.03 N/m, Neuchatel, Switzerland) was functionalized with fibronectin (50 μg/mL) for 30 minutes at 37°C. Suspensions of Caco-2 cells then were added into a 35-mm glass-bottom culture dish (ibidi, GmbH, Martinsried, Germany). After positioning and approaching the cantilever tip, a Caco-2 cell was captured by enabling contact (1 nN force for 10 seconds), followed by cantilever retraction to allow adhesion for 15 minutes. To investigate cell–cell adhesive strength, the Caco-2 cell attached to the cantilever was applied to selected cells (pcENS or smooth muscle cells), and a compressive force (0.5 nN) was applied for 10 seconds, followed by no force for 2 minutes. The cantilever then was retracted and its deflection was recorded. Two force curves were obtained for each pair of interactions and the minimum of the force curve was extracted to quantify the detachment force required to separate the cells.

Isolation of TEC/ENS Adhesion Complex Proteins

Surface proteins of nonconfluent Caco-2 cells were biotinylated using the Pierce cell surface protein isolation kit (Thermo Scientific, Valtham, MA) following the manufacturer's recommendations. Briefly, after 2 washes with PBS (4°C) and biotinylation for 30 minutes at 4°C, the reaction was quenched according to the kit protocol. Biotinylated cells were detached mechanically with a cell scraper, collected, and centrifuged (500 g for 3 minutes at 4°C). After 1 wash with Tris-buffered saline, the cell pellet was lysed with ice-cold lysis buffer 1 (20 mmol/L Tris at pH 7.6, 150 mmol/L NaCl, 1% NP-40, 1% Na deoxycholate, 2 mmol/L $MgCl_2$, 20 μg/mL aprotinin, 1 μg/mL leupeptin, and 1 μg/mL pepstatin). After centrifugation and sonication, biotinylated proteins were coupled to magnetic beads coated with streptavidin (Dynabeads M-280; Invitrogen). After extensive washes with PBS, the beads were incubated with pcENS for 30 minutes at 37°C, then lysed in ice-cold lysis buffer 2 (20 mmol/L Tris at pH 7.6, 150 mmol/L NaCl, 1% NP-40, 2 mmol/L $MgCl_2$, 20 μg/mL aprotinin, 1 μg/mL leupeptin, and 1 μg/mL pepstatin). Beads were collected from the lysate using a magnetic separation stand to allow adhesion complex isolation. Adhesion complexes then were denatured and reduced in Laemmli buffer, and analyzed by Western blot (using stain-free precast gels from BioRad, Hercules, CA). Primary antibodies used for Western blot analysis were rabbit anti–N-cadherin (1:750, 24345; Abcam), and mouse anti-L1CAM (1:750, ab24345; Abcam).

Statistics

All data are shown as means ± standard error of the mean. The Wilcoxon matched-pairs log-rank test was performed to compare continuous variations between 2 groups for the experiments on pcENS. The Friedman test with a Dunn post-test was used to compare continuous paired variables between more than 2 groups. One-way analysis of variance with a Bonferroni test was used to compare continuous unpaired variables between more than 2 groups. Cell motility data were compared with a Mann–Whitney test. Statistics were performed using the Prism software package (Graphpad Prism, La Jolla, CA), version 5. All experiments were independently repeated at least 3 times, with at least 2 repeated measures for each experiment. A P value less than .05 was considered statistically significant.

Results

Enteric Neurons Are Part of the Tumor Microenvironment

To confirm that enteric neurons were present within the TEC microenvironment, we co-stained histologic sections from 5 locally advanced (T3) human primary colorectal adenocarcinomas using antibodies directed against neuron-specific β-tubulin III protein (Tuj) protein and EpCAM. We observed Tuj-positive cells distributed densely and homogeneously in the 5 colorectal tumors studied (Figure 1). At the tumor invasion front (Figure 1C and D), and in more inner regions (Figure 1A and B), confocal microscopy further showed that Tuj-positive cells were in very close proximity to EpCAM-positive cells (Figure 1B), some being immediately adjacent to each other (Figure 1D). This strongly suggested that enteric neurons and TECs engage in direct cell–cell contact.

TECs Preferentially Adhere to Enteric Nervous Structures

To assess whether TECs adhere to enteric nervous structures, single-cell suspensions of GFP-expressing Caco-2 TECs were added to pcENS. After 15, 30, and 60 minutes of incubation, cultures were washed, fixed, and stained for ENS cellular components. We quantified the proportion of GFP TECs located within 1 pixel from Tuj-positive enteric nerve cells. To simplify, we use the term *juxtapose* to indicate immediate adjacent location throughout this report. Caco-2 suspension density was chosen so that GFP-positive cell area corresponded to only 1%–2% of the total well area (Figure 2A, B, E, and F). pcENS were composed of the 2 ENS cell types, enteric neurons (Tuj positive) and glial cells (S-100β positive), both lying on top of a layer of mesenchymal cells expressing the marker α-SMA (Figure 2A, C, E, and F). Strikingly, even though enteric neurons and glial cells covered a relatively minor area in pcENS wells (Figure 2A, C, E, and F), the majority (80%) of TECs were juxtaposed to Tuj-positive cellular structures as early as 15 minutes after TEC addition to pcENS cultures. This high percentage persisted at 30 minutes and 1 hour (Figure 2D). To evaluate adhesion strength between TECs and pcENS, Caco-2 cells attached to the cantilever of an

atomic force microscope (AFM) were applied until adhesive contact with the pcENS was achieved, and then the cantilever was lifted to detach the 2 cells (Figure 3A). AFM data quantifying the detachment force showed that adhesion strength was significantly higher between TECs and enteric nervous structures compared with TECs and A7R5 cells, used here as a prototypical mesenchymal cell type (Figure 3B).

To determine whether preferential adhesion to enteric nervous structures was a tumor cell–specific characteristic, we tested whether IEC6, a nontransformed intestinal epithelial cell line, had a different affinity for ENS structures compared with colorectal cancer Caco-2 cells. Adhesion tests showed that the proportion of nontransformed intestinal epithelial cells adhered to enteric neurons was slightly but significantly lower than TECs (Figure 4A–D). These data combined with the fact that in a healthy colon enteric neurons are in proximity to intestinal epithelial cells but remain physically separated by the basement membrane,[11,29] may suggest that cell–cell adhesion between enteric nervous structures and epithelial cells is more likely to involve TECs than normal epithelial cells.

Preferential Adhesion of TECs to Enteric Nervous Structures Specifically Involves Enteric Neurons

We next sought to determine the respective involvement of glial cells and enteric neurons in the physical interactions between TEC and ENS structures. In our in vitro model of pcENS co-cultured with TECs, confocal microscopy showed that TECs can directly engage enteric neurons without involving enteric glial cells (Figure 5A and Supplementary Video 1). Importantly, to assess the specific involvement of enteric neurons in TEC adhesion to ENS structures, we used primary cultures enriched for enteric neurons.[27] These cultures of enteric neurons are composed of 83% enteric neurons, 11% myofibroblasts, and do not contain any enteric glial cells. Results showed that despite the absence of enteric glial cells, more than 80% of TECs still were found adhered to enteric neurons (Figure 5B–E).

We next determined whether enteric neurons were required for adhesion between TEC and ENS structures. To test this, enteric neurons were removed from pcENS by successive passaging (Figure 5F and G), then TEC adhesion to pcENS depleted or not for enteric neurons was evaluated. Neuron depletion of pcENS led to a drastic decrease in TEC adhesion (7 ± 12 cells/mm^2 on neuron-depleted pcENS vs 59 ± 27 cells/mm^2 on neuron-containing pcENS) (Figure 5H, I, and K). To define the role of glial cells in TEC adhesion to ENS structures, we tested TEC adhesion to glial cells isolated from pcENS.[16] The percentage of TEC adhesion to enteric glial cells was strikingly lower compared with pcENS (25 ± 8 cells/mm^2 on enteric glial cells vs 59 ± 27 cells/mm^2 on pcENS control) (Figure 5H, J, and K). These results strengthen our findings that enteric neurons are the primary ENS cell type involved in TEC/ENS adhesion.
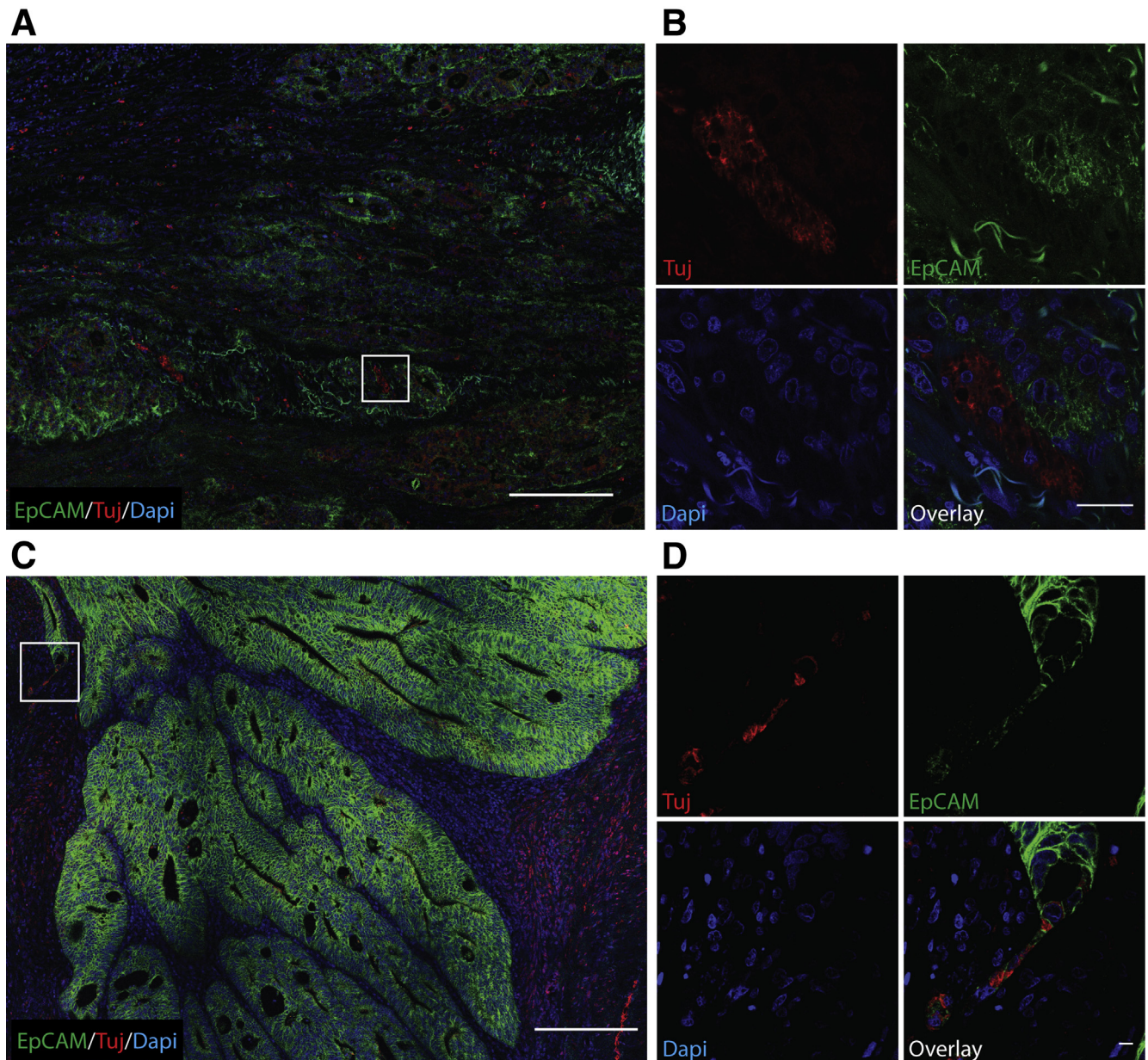
Figure 1. Enteric neurons are part of the tumor microenvironment. (*A* and *C*) Representative photographs of human colorectal adenocarcinoma sections immunostained for the neuronal marker β-tubulin III (red) and the epithelial marker EpCAM (green) showing the (*A*) center of the tumor and the (*C*) tumor front, showing the presence of enteric neurons in the tumor microenvironment. *Scale bars*: 250 μm. (*B* and *D*) Higher-magnification confocal micrographs (*white boxed regions* from panels *A* and *C*), illustrating the close proximity between tumor epithelial cells and enteric nervous structures. *Scale bars*: 25 μm. (*B*) Of note, nonspecific autofluorescence signal is visible in the lower left and upper right corners. DAPI, 4′,6-diamidino-2-phenylindole.

TEC Migration Is Favored on Enteric Neuronal Structures

During cancer invasion, tumor cell adhesion to resident neighboring cells is a key event initiating and guiding the migration of tumor cells.[4,30] Therefore, we tested whether TEC adhesion to enteric neurons impacted TEC migration. Migration of RFP-expressing TECs on pcENS containing GFP-positive neurons was monitored for 12 hours using time-lapse acquisition (Figure 6*A* and Supplementary Video 2). Cell-tracking analysis showed significant increases in total

distance and in distance to origin covered by TECs adhered to ENS structures compared with TECs adhered to non-neural structures (Figure 6*B–D*), showing that adhesion to neural structures promotes TEC migration. Next, to determine whether TECs migrated specifically along neuronal fibers, the trajectory axis angle of a single TEC adhered to a neuronal fiber was compared with the absolute angle of the corresponding fiber. Our data showed that the TEC trajectory angle strongly correlated with the angle of the neuronal fiber with a slope of 1 (Figure 6*E*), indicating that TECs
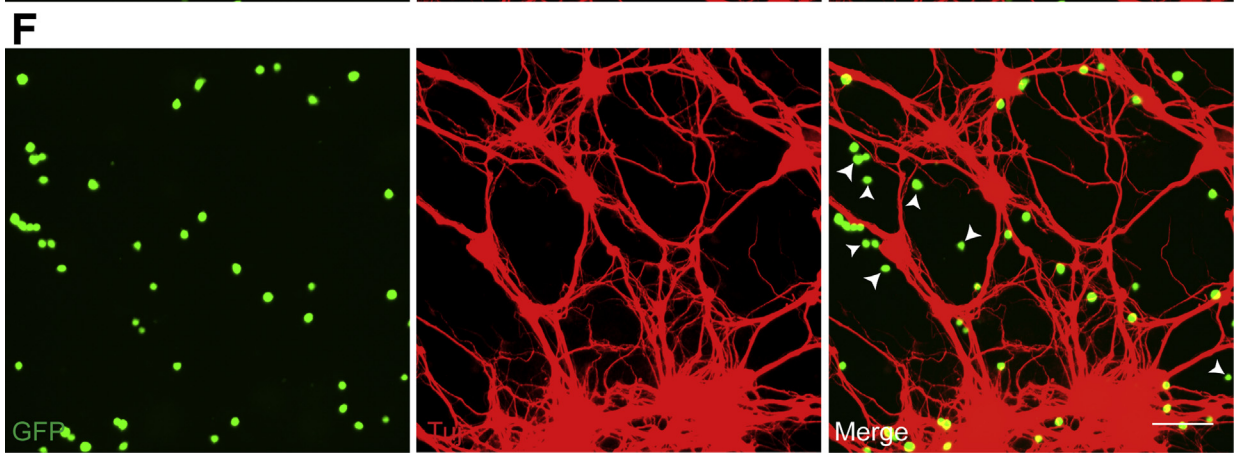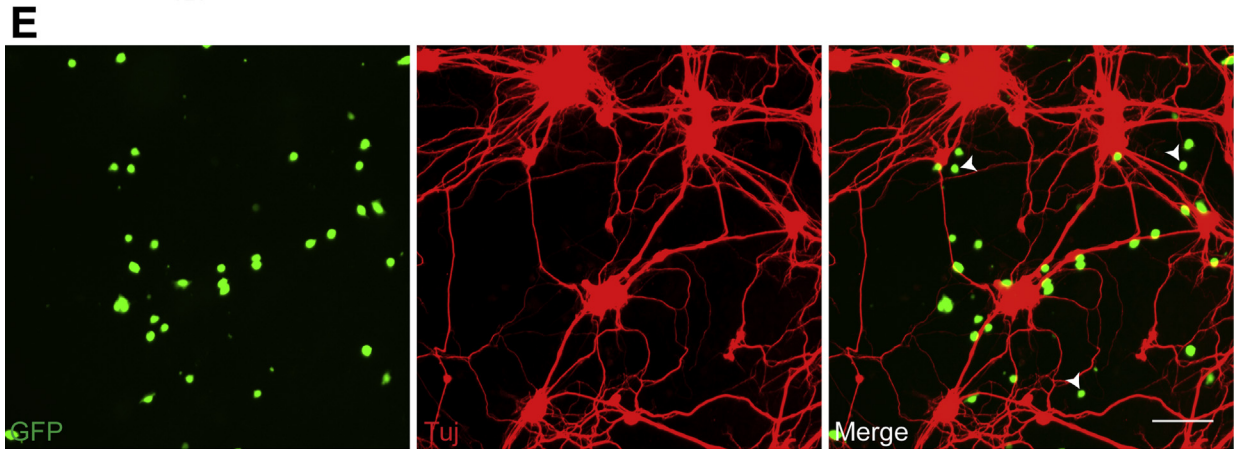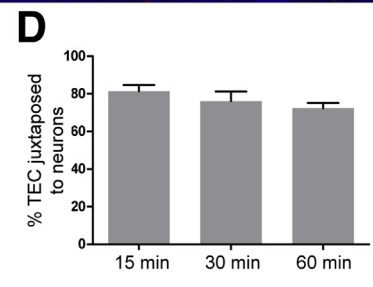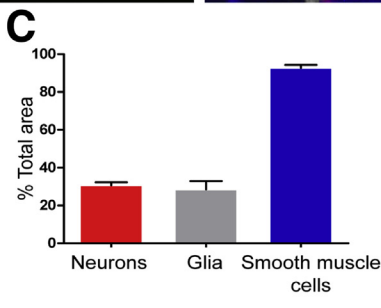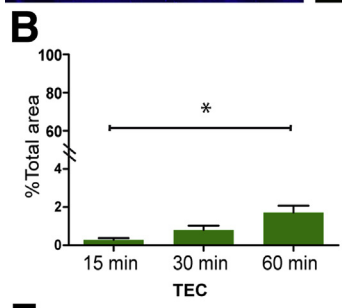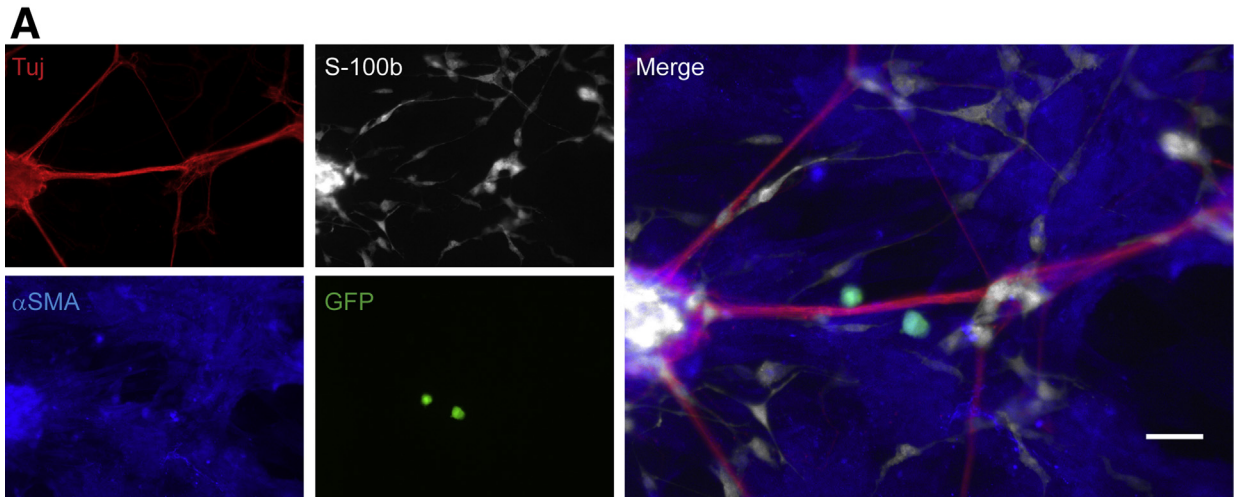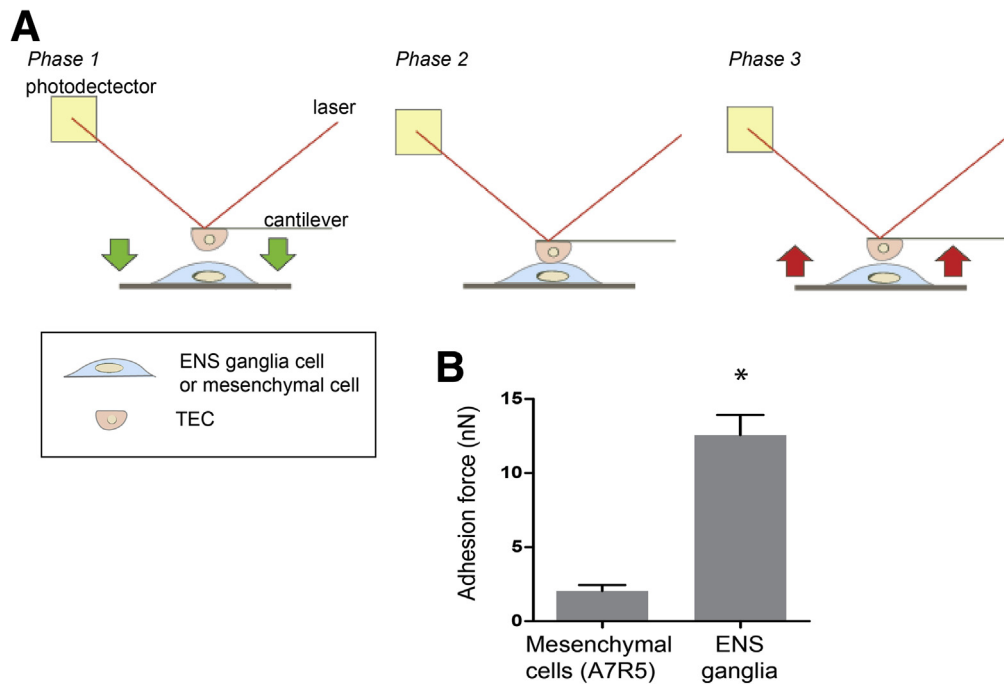
Figure 3. TEC adhesion to ENS is stronger than TEC adhesion to mesenchymal cells. (*A*) Schematic diagram of the method used to quantify adhesion force between TECs and ENS or TECs and mesenchymal cells. The AFM was set in contact mode and a TEC was attached to the cantilever. *Left*: The cantilever was pulled down until contact between the TEC and the underlying substrate (either ENS ganglia or mesenchymal cells) was achieved (*middle*). *Right*: The cantilever then was lifted up to quantify the strength required to detach the TEC from the underlying substrate. (*B*) AFM-based measurements of adhesion strength between TECs and enteric nervous ganglia from pcENS (ENS ganglia) and between TECs and mesenchymal cells (rat smooth muscle cells A7R5) (n = 23 cells from 3 independent experiments; *P < .001; Mann–Whitney test).

faithfully followed the ENS fiber path. This shows that the ENS network can physically guide TEC migration.

TEC Adhesion and Migration Along Enteric Neurons Are Mediated in Part by ENS L1CAM and N-Cadherin

To identify the adhesion proteins involved in TEC/ENS adhesion, we developed a proteomics approach based on extracellular adhesion protein labeling and purification (Figure 7*A*). After extracellular protein biotinylation, TEC surface proteins were isolated using streptavidin-coupled magnetic beads. The resulting TEC protein-labeled beads then were incubated with pcENS to mimic TEC/ENS adhesion. After lysis, TEC/ENS adhesion complexes were isolated by magnetic separation of the beads, and protein electrophoresis was performed on the following fractions: (1) TEC protein-labeled beads alone, (2) TEC protein-labeled beads that were incubated with pcENS, and (3) pcENS alone. We reasoned that any proteins involved in TEC/ENS adhesion must be present both in lysates from TEC-labeled beads incubated with pcENS (fraction 2) and from pcENS alone (fraction 3). Five major bands were detected at 40–45 kilodaltons, 70–80 kilodaltons, 95–100 kilodaltons, 120–130 kilodaltons, and 200–220 kilodaltons (Figure 7*B*). Western blot data showed that N-cadherin (100 kilodaltons) and L1CAM (200–220 kilodaltons) were present in both the TEC protein-labeled bead fraction incubated with pcENS, as well as in the pcENS-alone fraction (Figure 7*C* and *D*). Of note, N-cadherin and L1CAM were not detected at significant levels in the lysates of TEC protein-labeled beads alone. This suggests that adhesion

Figure 2. (*See previous page*). TECs adhere mainly to enteric nervous structures. (*A–D*) Adhesion assays using single-cell suspensions of GFP-expressing human tumor epithelial Caco-2 cells added to rat pcENS were performed. (*A*) Immunostaining of adhesion assays 1 hour after the addition of TECs to confluent pcENS. Staining of pcENS cellular components using antibodies against β-tubulin III (Tuj) (red), S-100β (white), and α-SMA (blue) illustrates the organization of neurons, glial cells, and smooth muscle cells, respectively. GFP-expressing TECs are shown in green. *Scale bar*: 50 μm. (*B* and *C*) Quantification of the area covered by each cellular component present in the adhesion assays. Data are expressed as means ± SEM of the percentages relative to the total area of the well (n = 4 wells obtained from 3 independent experiments; *P < .01; Friedman test with Dunn post-test). (*D*) Percentages of TECs juxtaposed to Tuj-positive structures relative to total TEC number at 15, 30, and 60 minutes after addition of TEC suspensions onto pcENS (n = 4 wells obtained from 3 independent experiments). (*E* and *F*) Representative photographs of the adhesion assays at a low magnification to show the enteric neuronal network (β-tubulin III, red) in confluent pcENS 1 hour after the addition of single-cell suspensions of GFP-expressing TECs (green). *Arrowheads* indicate the small subset of TECs not juxtaposed to ENS structures. *Scale bars*: 100 μm.
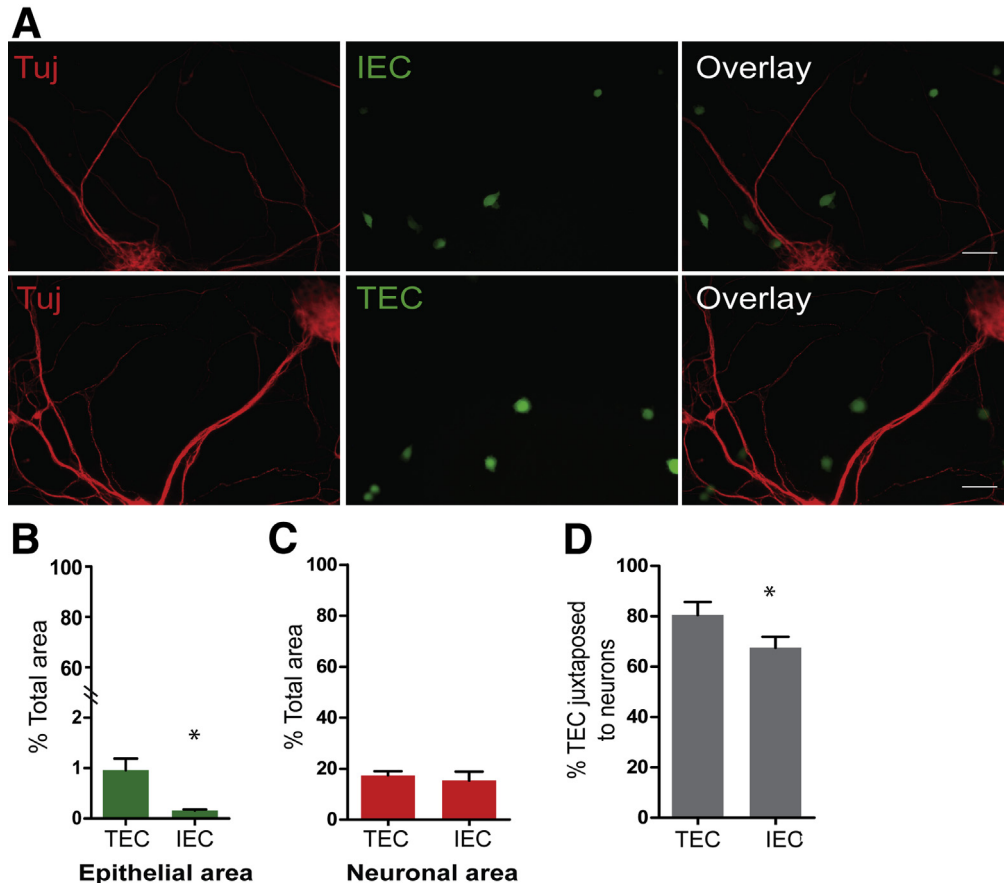
Figure 4. TECs adhere preferentially to ENS structures compared with normal intestinal epithelial cells. (A) Representative photographs of single-cell suspensions of nontransformed embryonic intestinal epithelial IEC-6 cells expressing FP635 (*upper panel*, IEC) and tumor epithelial Caco-2 cells expressing GFP (*lower panel*, TEC) incubated with pcENS for 1 hour. Epithelial cells and β-tubulin III–positive neuronal structures are shown in green and red, respectively. *Scale bars*: 50 μm. (B and C) Percentages of the (B) epithelial and (C) Tuj-positive neuronal areas relative to the total area of the well 1 hour after the addition of single-cell suspensions of TECs or IECs onto pcENS (n = 6 wells obtained from 3 independent experiments). (D) Quantification of the percentages of TECs and IECs juxtaposed to Tuj-positive structures relative to the total number of adhered TECs and IECs, respectively (n = 6 wells per condition obtained from 3 independent experiments; *P < .001; Mann–Whitney test).

complexes formed by ENS and TECs involve neuronal N-cadherin and L1CAM. Next, we confirmed that L1CAM and N-cadherin both were expressed by enteric neurons in pcENS by immunofluorescence microscopy (Figure 8A and C). Of note, L1CAM was not expressed by enteric glial cells in pcENS (Figure 8B). N-cadherin was expressed mainly by enteric neurons, although a weak staining could be detected in a subset of enteric glial cells and in some mesenchymal cells (Figure 8D).

To confirm that L1CAM and N-cadherin were present at adhesion sites between TECs and enteric neurons, immunostaining was performed after a 1-hour incubation of TEC suspensions with pcENS. Confocal microscopy showed that L1CAM was expressed by enteric neurons but not by TECs, and there was extensive recruitment of L1CAM at TEC/enteric neuron adhesion sites (Figure 9A). Confocal microscopy of N-cadherin showed that it was expressed on both TECs and enteric neuron cell surfaces at the adhesion site as well as in the adjacent area (Figure 9B). N-cadherin

immunostaining was slightly more enriched at the TEC edge involved in cell–cell contact. These results confirm that N-cadherin and L1CAM are present at adhesion sites between enteric neurons and TEC.

To test the functional implication of L1CAM and N-cadherin in TEC/ENS adhesion, pcENS were preincubated with selective L1CAM and N-cadherin blocking antibodies for 30 minutes before adding the TEC suspension. Blocking antibodies slightly but significantly decreased the proportion of TECs adhered to ENS structures (79% ± 16% vs 75% ± 19%; P = .03) (Figure 9C), providing further evidence that L1CAM and N-cadherin are involved in TEC adhesion to enteric nervous structures. Next, we tested L1CAM and N-cadherin involvement in TEC migration along neuronal fibers by performing time-lapse imaging in the presence of both blocking antibodies. Our results showed that the distance to origin but not the total distance covered by TECs was decreased markedly in the presence of L1CAM and N-cadherin blocking antibodies as compared with control
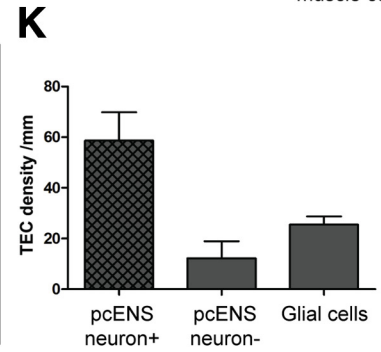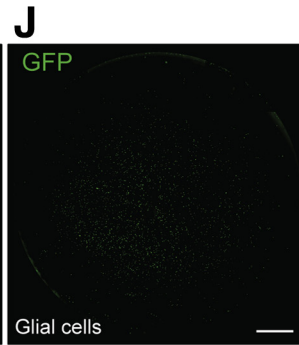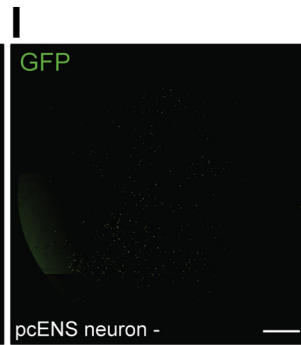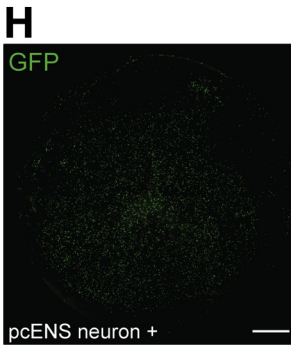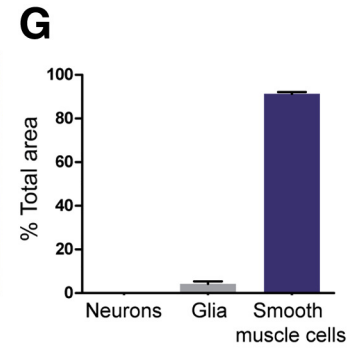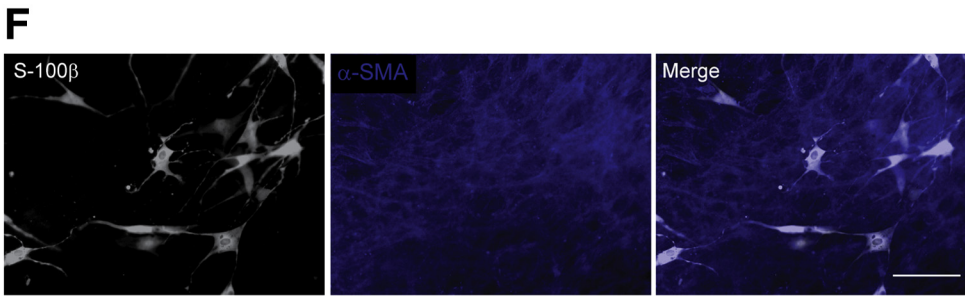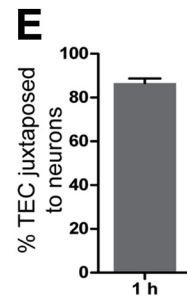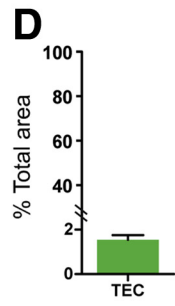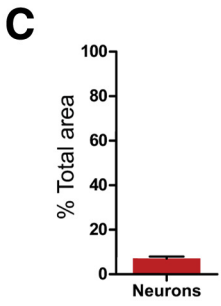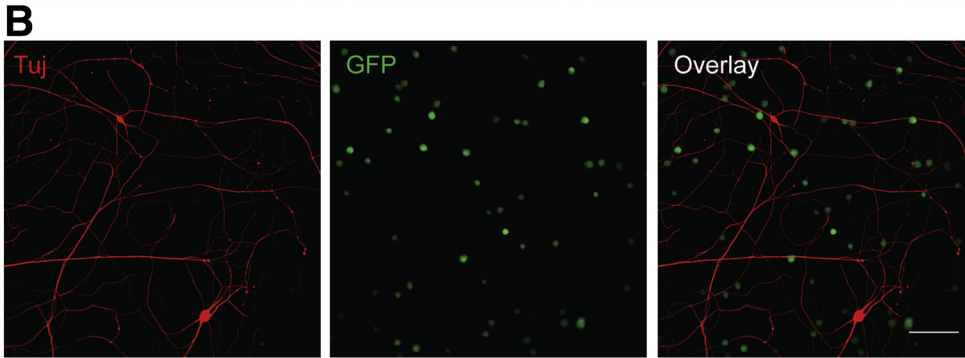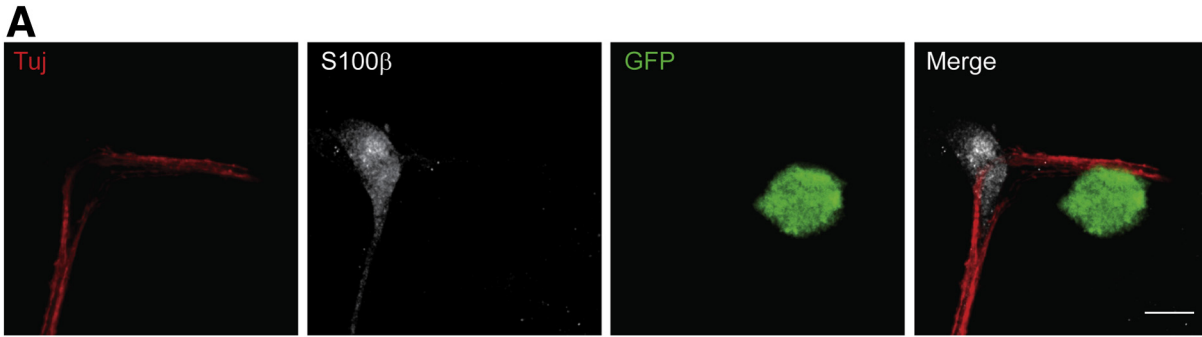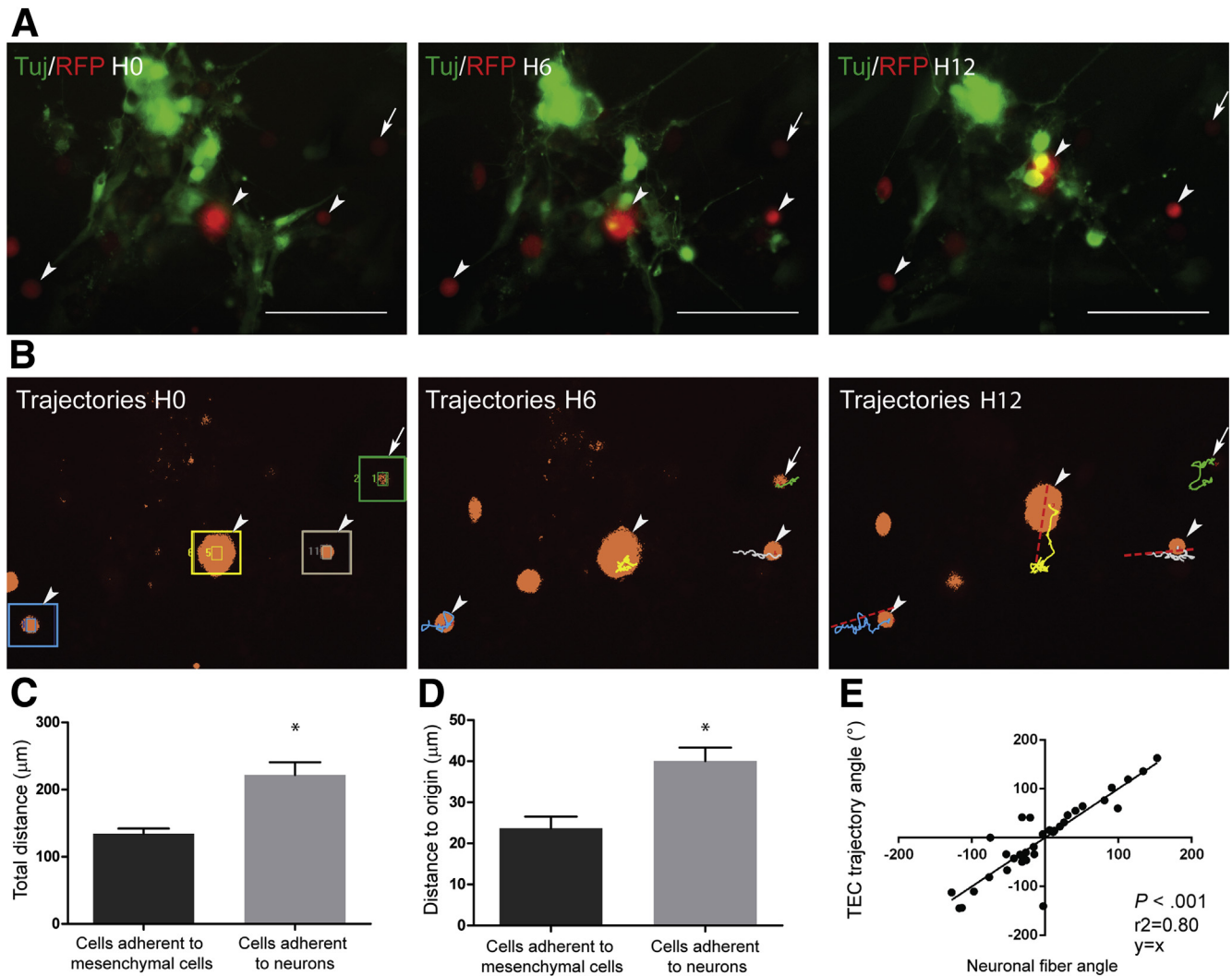
Figure 6. TEC preferential adhesion to enteric neurons guides TEC migration along ENS fibers. (A) Representative photographs at hour 0 (H0), H6, and H12 after incubating single-cell suspensions of TECs expressing RFP (red) with pcENS containing GFP-expressing neurons (green). *Scale bars*: 100 μm. (B) Modeling of the TEC trajectories using a cell-tracking method. (A and B) *Arrowheads* and *arrows* show TECs juxtaposed and nonjuxtaposed to enteric neuronal structures, respectively. (C and D) Measurement of (C) total distance and (D) distance to origin traveled by TECs juxtaposed to enteric neuron structures and to non-neuronal structures (mesenchymal cells) (n = 22 cells obtained from 3 independent experiments; *$P < .01$ Mann–Whitney test). (E) Linear regression testing the relationship between the angle of the TEC trajectory and the angle of the enteric nervous structure showed a highly significant correlation with a slope of 1 (n = 22 cells obtained from 3 independent experiments; *$P < .001$, $r^2 = 0.80$).

Figure 5. (*See previous page*). TEC adhesion to enteric nervous structures involves enteric neurons. (A) Confocal imaging of GFP-positive TECs adhered to pcENS showing intimate cell–cell contact between a TEC (green/GFP) and a neuronal projection (red/Tuj) without involving any enteric glial cell (white/S-100β). *Scale bar*: 10 μm. (B and E) Adhesion assays using single-cell suspensions of GFP-expressing human Caco-2 TECs and primary cultures of enteric neurons. (B) Representative photographs of enteric neurons (red/Tuj) after a 1-hour incubation with GFP-positive TEC suspension (green). *Scale bar*: 50 μm. (C and D) Percentages of (C) Tuj-positive neuronal area and (D) GFP-positive TEC area relative to total area of the well (n = 4 wells obtained from 3 independent experiments). (E) Percentage of TECs juxtaposed to enteric neurons relative to the total number of TECs (n = 4 wells obtained from 3 independent experiments). (F) Immunostaining for S-100β (white) and α-SMA (blue) in pcENS after removal of neural cells to show the presence of glial cells and smooth muscle cells, respectively. The absence of cells immunoreactive for β-tubulin III and Hu (pan-neuronal markers) confirmed the absence of neurons in pcENS after 2 successive passages. (G) Quantification of the area covered by each cellular component in pcENS after 2 successive passages. Data are expressed as means $\pm$ SEM of the percentages relative to the total area of the well (n = 3 wells obtained from 3 independent experiments). (H–K) TEC adhesion to pcENS depleted of neurons (pcENS neuron-) or not (pcENS neurons+), or to enteric glial cell cultures (glial cells). (H–J) Representative photographs of GFP-positive TECs (green) adhered to (H) pcENS neuron+, (I) pcENS neurons-, and (J) enteric glial cell culture after 15 minutes. *Scale bar*: 200 μm. (K) Density of TECs adhered to indicated cell cultures. Data are expressed as means $\pm$ SEM of TEC numbers per mm^2 (n = 6 wells per condition obtained from 3 independent experiments; *$P < .05$; 1-way analysis of variance with Bonferroni correction).
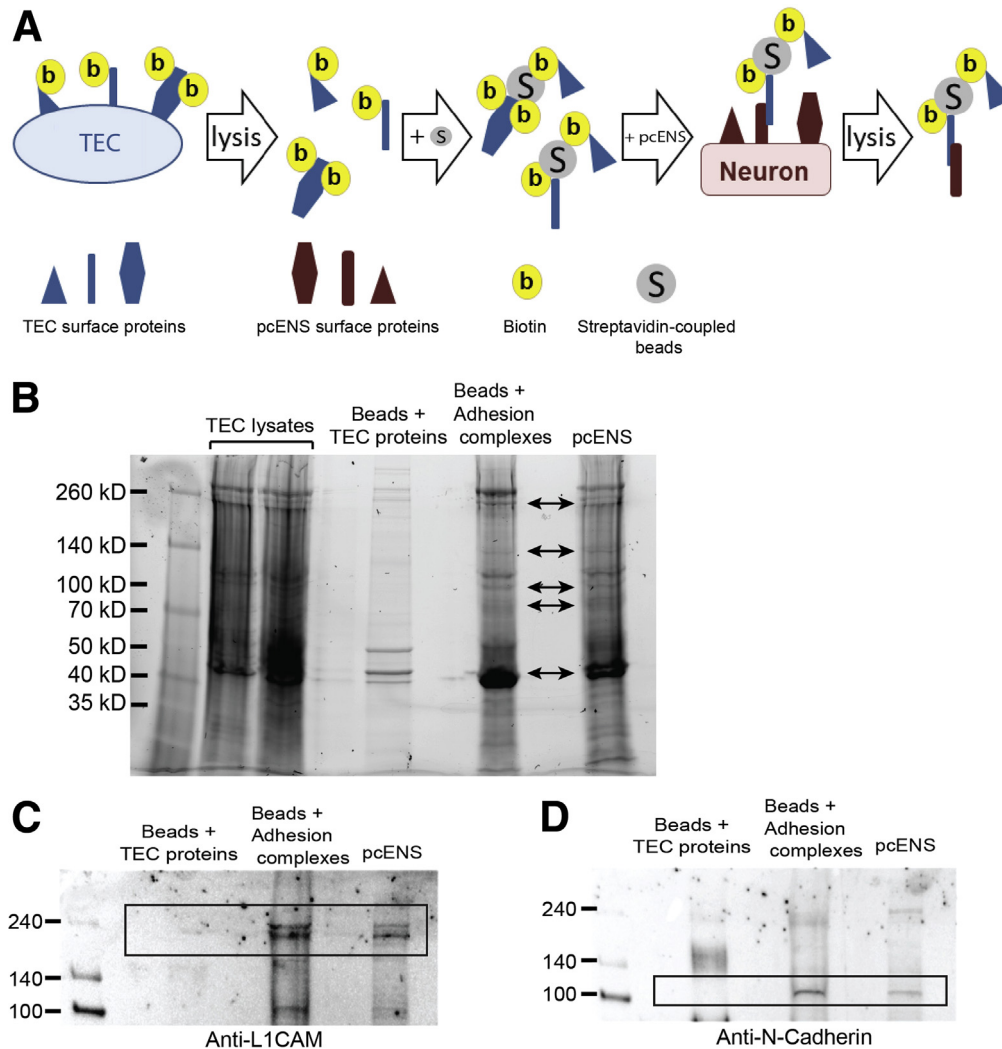
Figure 7. Neuronal adhesion proteins L1CAM and N-cadherin are present in the adhesion complexes between TECs and enteric nervous structures. (*A*) Schematic diagram showing the biochemical approach used to identify the proteins involved in TEC adhesion to enteric nervous structures. (*B*) Representative electrophoresis of TEC alone (TEC lysates), TEC protein-labeled beads (beads + TEC proteins), TEC protein-labeled beads incubated with pcENS (beads + adhesion complexes), and pcENS alone (pcENS). *Arrows* indicate the bands common to beads + adhesion complexes and pcENS fractions. Proteins common between these 2 fractions correspond to neural adhesion proteins mediating the adhesion complexes between TECs and pcENS (n = 2 experiments). (*C* and *D*) Representative Western blots showing the presence of (*C*) L1CAM and (*D*) N-cadherin in the lysate of the TEC protein-labeled beads incubated with pcENS (beads + adhesion complexes) and in the lysate of pcENS alone (pcENS) (n = 3 experiments).

(28 ± 19 μm vs 40 ± 24 μm; P < .01) (Figure 9*D* and *E*). Altogether, these data show that L1CAM and N-cadherin are involved in TEC adhesion and migration guidance on ENS structures.

Adhesion Assays Using Human Explant Cultures of Submucosal Plexus and Human Primary Colorectal Cancer Cells Confirmed Preferential Adhesion of TECs to ENS Plexus

Finally, we sought to validate our main findings using human primary specimens. We first tested whether single-cell suspensions of GFP-expressing TECs were able to physically interact with ex vivo explant cultures of human ENS

submucosal plexus (Figure 10*A* and Supplementary Video 3) (n = 3 explants). Immunostaining of submucosal enteric neurons (Tuj positive) and enteric glial cells (S-100β positive) showed that GFP-expressing TECs were able to adhere directly to cells of the ENS submucosal plexus. Next, we assessed whether TECs freshly isolated from T3 human primary colorectal adenocarcinomas preferentially adhered to neural structures in pcENS (Figure 10*B*–*E*). Quantification showed that as early as 4 hours after starting the coculture, a significant majority of human primary TECs (EpCAM positive) were juxtaposed to ENS structures. To validate our in vitro observations on L1CAM and N-cadherin involvement in adhesion between TECs and enteric neurons, we studied N-cadherin and L1CAM expression in human colorectal cancer
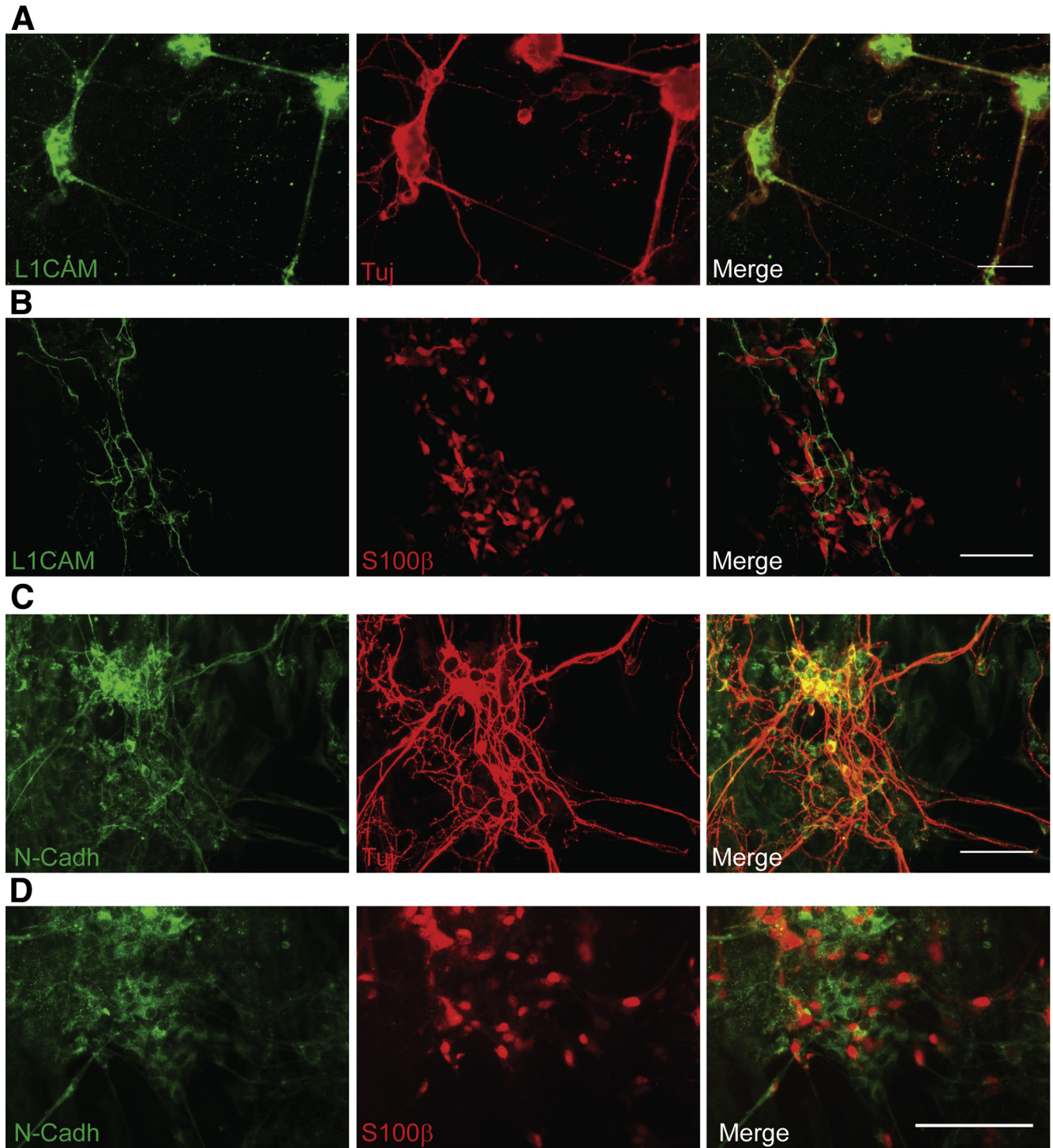
Figure 8. L1CAM and N-cadherin (N-Cadh) are both expressed by enteric neurons in pcENS. Immunostaining for (*A* and *B*) L1CAM and (*C* and *D*) N-cadherin in pcENS show that (*A*) L1CAM is expressed in enteric neurons (red/Tuj) but not in (*B*) enteric glial cells (red/S-100β), and that (*C*) N-cadherin is strongly expressed in enteric neurons (red/Tuj) as well as in (*D*) a subset of enteric glial cells (red/S-100β). *Scale bars*: 100 μm.

specimens by immunofluorescence. Staining of T3 human colorectal adenocarcinoma sections confirmed that enteric neurons strongly and selectively expressed L1CAM at adhesion sites with TECs (Figure 10*F*). N-cadherin immunostaining confirmed that both EpCAM-positive cancer cells and Tuj-positive enteric neurons expressed N-cadherin (Figure 10*G*). Altogether, these results using different human ex vivo models confirmed that human cancer epithelial cells preferentially adhere to ENS structures composed of enteric neurons positive for L1CAM and N-cadherin.
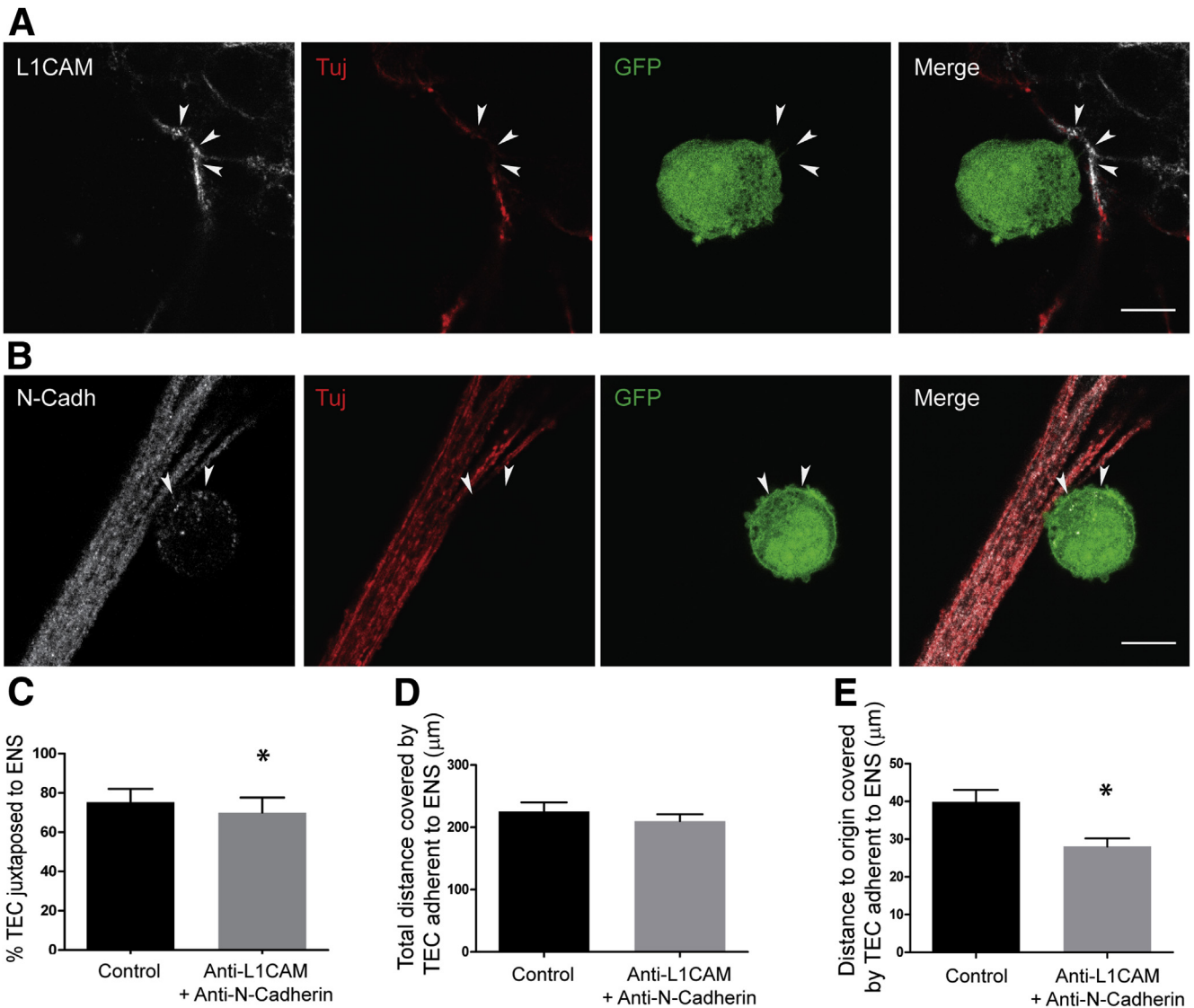
Figure 9. TEC adhesion and migration along enteric nervous structures are in part mediated by L1CAM and N-cadherin. (*A*) Representative images of L1CAM immunostaining (white) in pcENS (neurons/red/Tuj) after a 60-minute incubation with GFP-positive TEC suspension (green). *Arrowheads* show a strong signal for neuronal L1CAM at adhesion sites between TECs and neuronal structures. *Scale bar*: 10 μm. (*B*) Immunostaining for N-cadherin (N-Cadh) (white) in pcENS (neurons/red/Tuj) after a 60-minute incubation with GFP-positive TEC suspension (green). *Arrowheads* show more intense N-cadherin staining on TEC surface at adhesion site and at the immediately adjacent cell surface. *Scale bar*: 10 μm. (*C*) Percentages of the area covered by TECs juxtaposed to pcENS (relative to total TEC area) in the presence of blocking antibodies against L1CAM and N-cadherin, or control isotype (n = 6 wells obtained from 3 independent experiments, *P = .02; 1-way analysis of variance with the Dunn post-test). (*D* and *E*) Analyses of video-imaging using a cell-tracking method showed that although simultaneously blocking L1CAM and anti–N-cadherin had (*D*) no impact on total distance migrated, (*E*) it significantly decreased the distance to origin covered by TECs along nervous structures compared with control isotype antibodies (n = 56 cells obtained from 3 independent experiments; *P = .04; Mann–Whitney test).

Discussion

Until now, perineural invasion has been defined primarily in terms of physical interactions between tumor cells and Schwann cells of the peripheral extrinsic nerves, which guide the migration and proliferation of tumor cells by bringing them closer to sites of neuromediator and growth factor release.[5,22] Here, we show that in colorectal cancer, local intrinsic nervous structures that compose the ENS, provide the physical support for tumor cell docking and migration despite the absence of Schwann cells and myelin. Furthermore, consistent with previous findings, our confocal data on human primary colorectal adenocarcinomas confirm that enteric neurons are an abundant part of the colorectal cancer microenvironment.[31–33] Importantly, our study shows direct and strong physical interactions between tumor cells and ENS structures. Our adhesion assays showed the following: (1) a significant majority of TECs had increased affinity for neural structures in pcENS, (2)
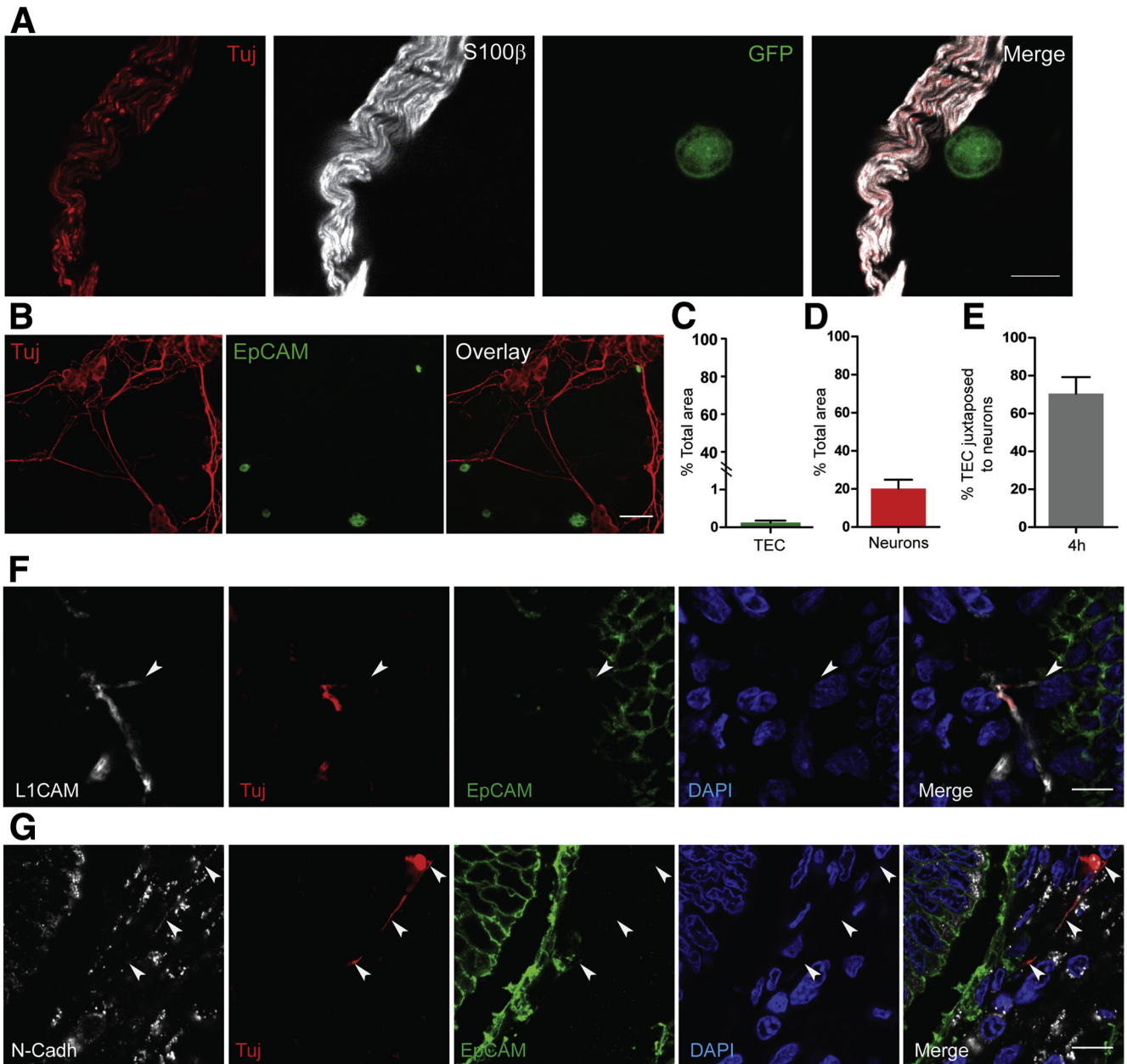
Figure 10. Adhesion assays using primary human TECs and explants of human submucosal plexus confirmed TEC preferential adhesion to ENS structures. (*A*) Representative confocal images of ex vivo microdissected human submucosal plexus composed of enteric neurons (red/β-tubulin III [Tuj]) and enteric glial cells (white/S-100β) after a 4-hour incubation with single-cell suspension of GFP-positive (green) Caco-2 TECs to show direct physical interactions between TECs and enteric nervous structures. *Scale bar*: 10 μm. (*B*) Representative images of single-cell suspensions of primary/native TECs isolated from human primary colon adenocarcinomas, incubated with pcENS for 4 hours, and immunostained for β-tubulin III in red and EpCAM in green. *Scale bar*: 50 μm. (*C* and *D*) Quantification of the area covered by (*C*) primary human colorectal cancer cells (TECs) and (*D*) neurons in adhesion assays (n = 6 wells obtained from 3 independent experiments). (*E*) Percentage of primary human colorectal cancer cells juxtaposed to Tuj-positive structures relative to total cancer cell number (n = 6 wells obtained from 3 independent experiments). (*F*) Immunostaining for L1CAM (white) at the tumor front of human colon adenocarcinomas (red/Tuj, green/EpCAM, and blue/nuclei/4′,6-diamidino-2-phenylindole [DAPI]). *Arrowhead* shows adhesion area between TECs and neuronal structures. *Scale bar*: 10 μm. (*G*) Immunostaining for N-cadherin (white) at the tumor front of human colon adenocarcinomas (white/Tuj, green/EpCAM, and blue/nuclei/DAPI). *Arrowheads* show adhesion areas between TECs and neuronal structures. *Scale bar*: 10 μm.

TEC adhesion to pcENS was decreased drastically by the depletion of neurons from the culture, and (3) adhesion strength (directly measured by AFM) was markedly higher between TECs and ENS than between TECs and mesenchymal cells. Preferential TEC adhesion to neural cells vs mesenchymal cells was confirmed using primary/native

human TECs and explant cultures of human ENS. Altogether, these results strongly suggest that enteric neurons are the predominant adhesion partner of tumor cells in the colorectal cancer microenvironment. Mesenchymal cells of the tumor microenvironment, often functionally grouped under the term *cancer-associated fibroblasts*, traditionally are seen as one of the most important cell types for physical guidance during the local migration of tumor cells.[6] However, our study highlights the fact that intrinsic neural cells also are privileged partners for tumor cell docking and migration.

Interestingly, previous studies of other cancer types have highlighted the role of Schwann cells in attracting tumor cells toward nerves.[5,22] Future studies will investigate which cell type of the ENS can attract TECs in the context of colorectal cancer. It is tempting to hypothesize that resident enteric glial cells might share this functional characteristic with Schwann cells because these 2 cell populations show similarities in gene expression profiles.[34] In light of our data, one might speculate that once tumor cells have been attracted by glial cells, neurons may be responsible for sustaining physical interactions with tumor cells and guiding their migration along the ENS network.

By using a novel proteomics approach based on extracellular adhesion protein labeling and purification, we found that TEC adhesion and migration along enteric neurons involved the neuronal molecules N-cadherin and L1CAM. Neurons were the only component of the ENS to express these 2 proteins. N-cadherin was expressed in both TECs and enteric neurons, suggesting homophilic interactions. Based on our immunofluorescence data, L1CAM was not expressed in tumor cells. This is consistent with previous reports showing that only 68% of colorectal cancers express L1CAM and that it is located preferentially in the less-differentiated cells at the tumor-invasive front[35,36]; thereby increasing the odds to study an L1CAM-negative area in human primary colon adenocarcinomas. Moreover, because L1CAM was expressed in enteric neurons but not in TECs, this indicates that neuronal L1CAM is involved in adhesion between TECs/enteric neurons via heterophilic interactions. Among known L1CAM heterophilic binding partners, integrins are of particular interest because they play a key role during epithelial-mesenchymal transition. Indeed, integrins are overexpressed during epithelial-mesenchymal transition, and they facilitate interactions between cells and the extracellular matrix to promote cell migration.[37–39] Previous studies in other organs have shown that L1CAM binding to $\alpha5\beta1$-integrin potentiated integrin-dependent cell migration via ERK1/2 activation.[40] These data suggest that integrins might be the putative heterophilic binding partners of neuronal L1CAM in the context of TEC/enteric neuron physical contact. Furthermore, our results show that simultaneously blocking L1CAM and N-cadherin slightly decreased TEC adhesion to enteric neurons, but strongly inhibited TEC migration along enteric neuronal fibers. Cell migration involves the dynamic formation of cell-substrate adhesion complexes to generate the adhesive forces required for cell traction.[41] The observation that blocking L1CAM and N-cadherin only slightly decreases tumor cell adhesion suggests that L1CAM and N-cadherin

are presumably not the predominant proteins involved in tumor cell adhesion on the ENS. On the other hand, the 25% decrease in tumor cell migration induced by blocking L1CAM and N-cadherin suggests that L1CAM and N-cadherin binding are involved in activating cell migration pathways.

In our model, TECs covered 450 μm/day (total distance), with an average distance-to-origin of 80 μm/day when migrating along the ENS. This velocity is consistent with and even greater than previous studies observed using in vitro models of perineural invasion; for example, pancreatic tumor cells migrating along neurites of dorsal root ganglia had an average velocity of 20–35 μm/day.[42] Furthermore, our data show that the TEC trajectory angle correlated with the angle of the neuronal fiber with a slope of 1. Together with our AFM data showing that TECs adhere to ENS structures with sufficient force to maintain stable direct interactions with enteric neurons, these findings support a model in which neuronal fibers can serve as a physical support and guidance scaffold for TEC migration. Interestingly, a similar mode of migration has been described during neuronal development. Immature neurons migrate along radial glial fibers from their birth place to their final cerebral destination, using a specific locomotion mode called "scaffold cell-dependent migration," which permits long distance and oriented dragging.[43] In neuronal development, scaffold cell-dependent migration is mediated by intracellular trafficking of N-cadherin, involving Rab5-dependent endocytosis and Rab11-dependent recycling of N-cadherin to the plasma membrane at the migration front. The result of this trafficking pathway is a shift of the N-cadherin homophilic complex toward the migration front.[44,45] Here, we show that N-cadherin is strongly expressed in enteric neurons. Consistent with previous studies,[46] we found that N-cadherin also was present on the TEC surface with a marked concentration immediately adjacent to sites of adhesion with neuronal cells. Because our data show that N-cadherin is involved in TEC migration along neuronal fibers, and to a lesser extent in TEC/ENS adhesion, it is tempting to speculate that TECs migrate using an N-cadherin–mediated scaffold cell-dependent migration mode using enteric neurons as scaffold cells.

For a long time, perineural invasion has been considered relevant for colorectal cancer prognosis, mainly when it was observed beyond the muscularis propria.[47] However, recent studies have shown that perineural invasion within the myenteric plexus of the ENS is correlated inversely with disease-free survival in colorectal cancer.[9] Here, we provide strong evidence supporting the idea that the ENS, and specifically the enteric neurons expressing L1CAM and N-cadherin, physically guide the migration of colorectal cancer cells. In future studies, it will be interesting to determine if perineural invasion involving extrinsic nerves beyond the muscularis propria is a continuation of invasion initiated in plexi of the intrinsic ENS, and whether it involves similar adhesion molecules. In addition, future work will test whether the neuronal expression of L1CAM and N-cadherin in the tumor microenvironment also inversely correlates with prognosis in colorectal cancer. This

hypothesis is supported by previous studies in pancreatic cancer, in which L1CAM expression is associated significantly with perineural invasion incidence.[48] From a therapeutic perspective, neuronal N-cadherin, L1CAM, and their adhesion partners on the tumor cell surface constitute potential targets to limit colorectal cancer local dissemination.

Conclusions

In this study, we show that TECs can adhere to and migrate along neuronal fibers. Given the widespread extent of the ENS network and its multiple connections with the extrinsic nervous system, this ability could permit tumor cells to cover long distances and rapidly invade surrounding tissues. Moreover, several studies have shown that tumor cells induce neuritogenesis in the tumor microenvironment via the release of neurotrophic factors.[31,49,50] By increasing the density of the intrinsic neuronal network, tumor cells may multiply their potential invasion routes. Thus, greater knowledge of the physical guidance of tumor cells by the enteric neuronal network will allow a better understanding of the local progression of colorectal cancer.

References

1. Hanahan D, Coussens LM. Accessories to the crime: functions of cells recruited to the tumor microenvironment. Cancer Cell 2012;21:309–322.
2. Friedl P, Wolf K. Plasticity of cell migration: a multiscale tuning model. J Cell Biol 2010;188:11–19.
3. Roh-Johnson M, Bravo-Cordero JJ, Patsialou A, Sharma VP, Guo P, Liu H, Hodgson L, Condeelis J. Macrophage contact induces RhoA GTPase signaling to trigger tumor cell intravasation. Oncogene 2014; 33:4203–4212.
4. Friedl P, Alexander S. Cancer invasion and the microenvironment: plasticity and reciprocity. Cell 2011; 147:992–1009.
5. Deborde S, Omelchenko T, Lyubchik A, Zhou Y, He S, McNamara WF, Chernichenko N, Lee S-Y, Barajas F, Chen C-H, Bakst RL, Vakiani E, He S, Hall A, Wong RJ. Schwann cells induce cancer cell dispersion and invasion. J Clin Invest 2016;126:1538–1554.
6. Labernadie A, Kato T, Brugués A, Serra-Picamal X, Derzsi S, Arwert E, Weston A, González-Tarragó V, Elosegui-Artola A, Albertazzi L, Alcaraz J, Roca-Cusachs P, Sahai E, Trepat X. A mechanically active heterotypic E-cadherin/N-cadherin adhesion enables fibroblasts to drive cancer cell invasion. Nat Cell Biol 2017;19:224–237.
7. Liebig C, Ayala G, Wilks JA, Berger DH, Albo D. Perineural invasion in cancer: a review of the literature. Cancer 2009;115:3379–3391.
8. Liebig C, Ayala G, Wilks J, Verstovsek G, Liu H, Agarwal N, Berger DH, Albo D. Perineural invasion is an independent predictor of outcome in colorectal cancer. J Clin Oncol 2009;27:5131–5137.
9. Ueno H, Shirouzu K, Shimazaki H, Kawachi H, Eishi Y, Ajioka Y, Okuno K, Yamada K, Sato T, Kusumi T, Kushima R, Ikegami M, Kojima M, Ochiai A, Murata A, Akagi Y, Nakamura T, Sugihara K. Histogenesis and prognostic value of myenteric spread in colorectal cancer: a Japanese multi-institutional study. J Gastroenterol 2014;49:400–407.
10. Wedel T, Roblick U, Gleiss J, Schiedeck T, Bruch HP, Kühnel W, Krammer HJ. Organization of the enteric nervous system in the human colon demonstrated by whole-mount immunohistochemistry with special reference to the submucous plexus. Ann Anat 1999;181:327–337.
11. Neunlist M, Van Landeghem L, Mahé MM, Derkinderen P, des Varannes SB, Rolli-Derkinderen M. The digestive neuronal-glial-epithelial unit: a new actor in gut health and disease. Nat Rev Gastroenterol Hepatol 2013;10:90–100.
12. Gershon MD, Bursztajn S. Properties of the enteric nervous system: limitation of access of intravascular macromolecules to the myenteric plexus and muscularis externa. J Comp Neurol 1978;180:467–487.
13. Neunlist M, Van Landeghem L, Bourreille A, Savidge T. Neuro-glial crosstalk in inflammatory bowel disease. J Intern Med 2008;263:577–583.
14. Moriez R, Abdo H, Chaumette T, Faure M, Lardeux B, Neunlist M. Neuroplasticity and neuroprotection in enteric neurons: role of epithelial cells. Biochem Biophys Res Commun 2009;382:577–582.
15. Bach-Ngohou K, Mahé MM, Aubert P, Abdo H, Boni S, Bourreille A, Denis MG, Lardeux B, Neunlist M, Masson D. Enteric glia modulate epithelial cell proliferation and differentiation through 15-deoxy-12,14-prostaglandin J2. J Physiol 2010;588:2533–2544.
16. Van Landeghem L, Chevalier J, Mahé MM, Wedel T, Urvil P, Derkinderen P, Savidge T, Neunlist M. Enteric glia promote intestinal mucosal healing via activation of focal adhesion kinase and release of proEGF. Am J Physiol Gastrointest Liver Physiol 2011;300:G976–G987.
17. Van Landeghem L, Mahé MM, Teusan R, Léger J, Guisle I, Houlgatte R, Neunlist M. Regulation of intestinal epithelial cells transcriptome by enteric glial cells: impact on intestinal epithelial barrier functions. BMC Genomics 2009;10:507.
18. Flamant M, Aubert P, Rolli-Derkinderen M, Bourreille A, Neunlist MR, Mahé MM, Meurette G, Marteyn B, Savidge T, Galmiche JP, Sansonetti PJ, Neunlist M. Enteric glia protect against Shigella flexneri invasion in intestinal epithelial cells: a role for S-nitrosoglutathione. Gut 2011;60:473–484.
19. Marchesi F, Locatelli M, Solinas G, Erreni M, Allavena P, Mantovani A. Role of CX3CR1/CX3CL1 axis in primary and secondary involvement of the nervous system by cancer. J Neuroimmunol 2010;224:39–44.
20. Swanson BJ, McDermott KM, Singh PK, Eggers JP, Crocker PR, Hollingsworth MA. MUC1 is a counter-receptor for myelin-associated glycoprotein (Siglec-4a) and their interaction contributes to adhesion in pancreatic cancer perineural invasion. Cancer Res 2007; 67:10222–10229.
21. He S, Chen C-H, Chernichenko N, He S, Bakst RL, Barajas F, Deborde S, Allen PJ, Vakiani E, Yu Z, Wong RJ. GFRα1 released by nerves enhances cancer cell perineural invasion through GDNF-RET signaling. Proc Natl Acad Sci U S A 2014;111:E2008–E2017.

22. Demir IE, Boldis A, Pfitzinger PL, Teller S, Brunner E, Klose N, Kehl T, Maak M, Lesina M, Laschinger M, Janssen K-P, Algül H, Friess H, Ceyhan GO. Investigation of Schwann cells at neoplastic cell sites before the onset of cancer invasion. J Natl Cancer Inst 2014;106.

23. Ryschich E, Khamidjanov A, Kerkadze V, Büchler MW, Zöller M, Schmidt J. Promotion of tumor cell migration by extracellular matrix proteins in human pancreatic cancer. Pancreas 2009;38:804–810.

24. Ayala GE, Wheeler TM, Shine HD, Schmelz M, Frolov A, Chakraborty S, Rowley D. In vitro dorsal root ganglia and human prostate cell line interaction: redefining perineural invasion in prostate cancer. Prostate 2001;49:213–223.

25. Marchesi F, Piemonti L, Fedele G, Destro A, Roncalli M, Albarello L, Doglioni C, Anselmo A, Doni A, Bianchi P, Laghi L, Malesci A, Cervo L, Malosio M, Reni M, Zerbi A, Di Carlo V, Mantovani A, Allavena P. The chemokine receptor CX3CR1 is involved in the neural tropism and malignant behavior of pancreatic ductal adenocarcinoma. Cancer Res 2008;68:9060–9069.

26. Chevalier J, Derkinderen P, Gomes P, Thinard R, Naveilhan P, Vanden Berghe P, Neunlist M. Activity-dependent regulation of tyrosine hydroxylase expression in the enteric nervous system. J Physiol 2008; 586:1963–1975.

27. Le Berre-Scoul C, Chevalier J, Oleynikova E, Cossais F, Talon S, Neunlist M, Boudin H. A novel enteric neuron-glia coculture system reveals the role of glia in neuronal development. J Physiol 2017;595:583–598.

28. Liu L, Geisert EE, Frankfurter A, Spano AJ, Jiang CX, Yue J, Dragatsis I, Goldowitz D. A transgenic mouse class-III beta tubulin reporter using yellow fluorescent protein. Genesis 2007;45:560–569.

29. Mestres P, Diener M, Rummel W. Electron microscopy of the mucosal plexus of the rat colon. Acta Anat (Basel) 1992;143:275–282.

30. Kalluri R, Weinberg RA. The basics of epithelial-mesenchymal transition. J Clin Invest 2009; 119:1420–1428.

31. Albo D, Akay CL, Marshall CL, Wilks JA, Verstovsek G, Liu H, Agarwal N, Berger DH, Ayala GE. Neurogenesis in colorectal cancer is a marker of aggressive tumor behavior and poor outcomes. Cancer 2011; 117:4834–4845.

32. Fujita S, Nakanisi Y, Taniguchi H, Yamamoto S, Akasu T, Moriya Y, Shimoda T. Cancer invasion to Auerbach's plexus is an important prognostic factor in patients with pT3-pT4 colorectal cancer. Dis Colon Rectum 2007; 50:1860–1866.

33. Liebl F, Demir IE, Rosenberg R, Boldis A, Yildiz E, Kujundzic K, Kehl T, Dischl D, Schuster T, Maak M, Becker K, Langer R, Laschinger M, Friess H, Ceyhan GO. The severity of neural invasion is associated with shortened survival in colon cancer. Clin Cancer Res 2013; 19:50–61.

34. Rao M, Nelms BD, Dong L, Salinas-Rios V, Rutlin M, Gershon MD, Corfas G. Enteric glia express proteolipid protein 1 and are a transcriptionally unique population of glia in the mammalian nervous system. Glia 2015, Epub ahead of print.

35. Gavert N, Conacci-Sorrell M, Gast D, Schneider A, Altevogt P, Brabletz T, Ben-Ze'ev A. L1, a novel target of beta-catenin signaling, transforms cells and is expressed at the invasive front of colon cancers. J Cell Biol 2005; 168:633–642.

36. Gavert N, Vivanti A, Hazin J, Brabletz T, Ben-Ze'ev A. L1-mediated colon cancer cell metastasis does not require changes in EMT and cancer stem cell markers. Mol Cancer Res 2011;9:14–24.

37. Plotnikov SV, Waterman CM. Guiding cell migration by tugging. Curr Opin Cell Biol 2013;25:619–626.

38. Iwamoto DV, Calderwood DA. Regulation of integrin-mediated adhesions. Curr Opin Cell Biol 2015; 36:41–47.

39. Itoh K, Fushiki S, Kamiguchi H, Arnold B, Altevogt P, Lemmon V. Disrupted Schwann cell-axon interactions in peripheral nerves of mice with altered L1-integrin interactions. Mol Cell Neurosci 2005;30:624–629.

40. Thelen K, Kedar V, Panicker AK, Schmid R-S, Midkiff BR, Maness PF. The neural cell adhesion molecule L1 potentiates integrin-dependent cell migration to extracellular matrix proteins. J Neurosci 2002;22:4918–4931.

41. Schwartz MA, Horwitz AR. Integrating adhesion, protrusion, and contraction during cell migration. Cell 2006; 125:1223–1225.

42. Wang L, Zhi X, Zhu Y, Zhang Q, Wang W, Li Z, Tang J, Wang J, Wei S, Li B, Zhou J, Jiang J, Yang L, Xu H, Xu Z. MUC4-promoted neural invasion is mediated by the axon guidance factor Netrin-1 in PDAC. Oncotarget 2015; 6:33805–33822.

43. Nishimura YV, Sekine K, Chihama K, Nakajima K, Hoshino M, Nabeshima Y, Kawauchi T. Dissecting the factors involved in the locomotion mode of neuronal migration in the developing cerebral cortex. J Biol Chem 2010;285:5878–5887.

44. Kawauchi T. Cell adhesion and its endocytic regulation in cell migration during neural development and cancer metastasis. Int J Mol Sci 2012;13:4564–4590.

45. Jossin Y, Cooper JA. Reelin, Rap1 and N-cadherin orient the migration of multipolar neurons in the developing neocortex. Nat Neurosci 2011;14:697–703.

46. Yan X, Yan L, Liu S, Shan Z, Tian Y, Jin Z. N-cadherin, a novel prognostic biomarker, drives malignant progression of colorectal cancer. Mol Med Rep 2015; 12:2999–3006.

47. Goldstein NS, Turner JR. Pericolonic tumor deposits in patients with T3N+MO colon adenocarcinomas: markers of reduced disease free survival and intra-abdominal metastases and their implications for TNM classification. Cancer 2000;88:2228–2238.

48. Ben Q-W, Wang J-C, Liu J, Zhu Y, Yuan F, Yao W-Y, Yuan Y-Z. Positive expression of L1-CAM is associated with perineural invasion and poor outcome in pancreatic ductal adenocarcinoma. Ann Surg Oncol 2010;17:2213–2221.

49. Ayala GE, Dai H, Powell M, Li R, Ding Y, Wheeler TM, Shine D, Kadmon D, Thompson T, Miles BJ, Ittmann MM, Rowley D. Cancer-related axonogenesis and neurogenesis in prostate cancer. Clin Cancer Res 2008; 14:7593–7603.

50. Magnon C, Hall SJ, Lin J, Xue X, Gerber L, Freedland SJ, Frenette PS. Autonomic nerve development contributes to prostate cancer progression. Science 2013;341:1236361.

Author contributions
Emilie Duchalais, L. Van Landeghem, Christophe Guilluy, Hélène Boudin, and M. Neunlist conceived and designed the experiments; Emilie Duchalais, Melissa Touvron, and Christophe Guilluy performed the experiments with the help of Steven Nedellec for confocal microscopy and videoimaging and Guy Louarn for atomic force microscopy; Emilie Duchalais, Christophe Guilluy, and L. Van Landeghem analyzed the data; Céline Bossard and Emilie Duchalais collected the human colon specimens; and Emilie Duchalais, L. Van Landeghem, Christophe Guilluy, and M. Neunlist wrote the manuscript. All authors reviewed and approved the paper.